

ISSN 2523-2517

Volume 7, Issue 18 — January — June — 2023

Journal Electrical Engineering

ECORFAN[®]

ECORFAN-Peru

Editor in Chief

QUINTANILLA-CÓNDOR, Cerapio. PhD

Executive Director

RAMOS-ESCAMILLA, María. PhD

Editorial Director

PERALTA-CASTRO, Enrique. MsC

Web Designer

ESCAMILLA-BOUCHAN, Imelda. PhD

Web Designer

LUNA-SOTO, Vladimir. PhD

Editorial Assistant

TREJO-RAMOS, Iván. BsC

Philologist

RAMOS-ARANCIBIA, Alejandra. BsC

Journal Electrical Engineering, Volume 7, Issue 18, June, 2023, is a magazine published biannually by ECORFAN-Peru. La Raza Av. 1047 No. - Santa Ana, CuscoPeru. Postcode: 11500. WEB: www.ecorfan.org/republicofperu, revista@ecorfan.org. Editor in Chief: QUINTANILLA - CÓNDOR, Cerapio. PhD. ISSN: 2523-2517. Responsible for the last update of this issue of the ECORFAN Informatics Unit. ESCAMILLA-BOUCHÁN Imelda, LUNA-SOTO, Vladimir, updated June 30, 2023.

The views expressed by the authors do not necessarily reflect the views of the publisher.

The total or partial reproduction of the contents and images of the publication without the permission of the National Institute for the Defense of Competition and Protection of Intellectual Property is strictly prohibited.

Journal Electrical Engineering

Definition of Journal

Scientific Objectives

Support the international scientific community in its written production Science, Technology and Innovation in the Field of Engineering and Technology, in Subdisciplines Electromagnetism, electrical distribution sources, electrical engineering innovation, signal amplification, electric motor design, material science in power plants, management and distribution of electrical energies.

ECORFAN-Mexico, S.C. is a Scientific and Technological Company in contribution to the Human Resource training focused on the continuity in the critical analysis of International Research and is attached to CONAHCYT-RENIECYT number 1702902, its commitment is to disseminate research and contributions of the International Scientific Community, academic institutions, agencies and entities of the public and private sectors and contribute to the linking of researchers who carry out scientific activities, technological developments and training of specialized human resources with governments, companies and social organizations.

Encourage the interlocation of the International Scientific Community with other Study Centers in Mexico and abroad and promote a wide incorporation of academics, specialists and researchers to the publication in Science Structures of Autonomous Universities - State Public Universities - Federal IES - Polytechnic Universities - Technological Universities - Federal Technological Institutes - Normal Schools - Decentralized Technological Institutes - Intercultural Universities - S & T Councils - CONAHCYT Research Centers.

Scope, Coverage and Audience

Journal Electrical Engineering is a Research Journal edited by ECORFAN-Mexico S.C in its Holding with repository in Republic of Peru, is a scientific publication arbitrated and indexed with semester periods. It supports a wide range of contents that are evaluated by academic peers by the Double-Blind method, around subjects related to the theory and practice of Electromagnetism, electrical distribution sources, electrical engineering innovation, signal amplification, electric motor design, material science in power plants, management and distribution of electrical energies with diverse approaches and perspectives, That contribute to the diffusion of the development of Science Technology and Innovation that allow the arguments related to the decision making and influence in the formulation of international policies in the Field of Engineering and Technology. The editorial horizon of ECORFAN-Mexico® extends beyond the academy and integrates other segments of research and analysis outside the scope, as long as they meet the requirements of rigorous argumentative and scientific, as well as addressing issues of general and current interest of the International Scientific Society.

Editorial Board

GUZMÁN - ARENAS, Adolfo. PhD
Massachusetts Institute of Technology

LÓPEZ - BONILLA, Oscar Roberto. PhD
University of New York at Stony Brook

DE LA ROSA - VARGAS, José Ismael. PhD
Universidad París XI

FERNANDEZ - ZAYAS, José Luis. PhD
University of Bristol

LÓPEZ - HERNÁNDEZ, Juan Manuel. PhD
Institut National Polytechnique de Lorraine

MEDELLIN - CASTILLO, Hugo Iván. PhD
Heriot-Watt University

TIRADO - RAMOS, Alfredo. PhD
University of Amsterdam

VAZQUEZ - MARTINEZ, Ernesto. PhD
University of Manitoba

AYALA - GARCÍA, Ivo Neftalí. PhD
University of Southampton

DECTOR - ESPINOZA, Andrés. PhD
Centro de Microelectrónica de Barcelona

Arbitration Committee

TECPOYOTL - TORRES, Margarita. PhD
Universidad Autónoma del Estado de Morelos

CASTILLO - BARRÓN, Allen Alexander. PhD
Instituto Tecnológico de Morelia

GUDIÑO - LAU, Jorge. PhD
Universidad Nacional Autónoma de México

HERNÁNDEZ - NAVA, Pablo. PhD
Instituto Nacional de Astrofísica Óptica y Electrónica

TREJO - MACOTELA, Francisco Rafael. PhD
Instituto Nacional de Astrofísica, Óptica y Electrónica

HERNÁNDEZ - GÓMEZ, Víctor Hugo. PhD
Universidad Nacional Autónoma de México

HERRERA - ROMERO, José Vidal. PhD
Universidad Nacional Autónoma de México

SALINAS - ÁVILES, Oscar Hilario. PhD
Centro de Investigación y Estudios Avanzados -IPN

VASQUEZ - SANTACRUZ, J.A. PhD
Centro de Investigación y Estudios Avanzados

CASTILLO - TÉLLEZ, Margarita. PhD
Universidad Nacional Autónoma de México

Assignment of Rights

The sending of an Article to Journal Electrical Engineering emanates the commitment of the author not to submit it simultaneously to the consideration of other series publications for it must complement the Originality Format for its Article.

The authors sign the Authorization Format for their Article to be disseminated by means that ECORFAN-Mexico, S.C. In its Holding Republic of Peru considers pertinent for disclosure and diffusion of its Article its Rights of Work.

Declaration of Authorship

Indicate the Name of Author and Coauthors at most in the participation of the Article and indicate in extensive the Institutional Affiliation indicating the Department.

Identify the Name of Author and Coauthors at most with the CVU Scholarship Number-PNPC or SNI-CONAHCYT- Indicating the Researcher Level and their Google Scholar Profile to verify their Citation Level and H index.

Identify the Name of Author and Coauthors at most in the Science and Technology Profiles widely accepted by the International Scientific Community ORC ID - Researcher ID Thomson - arXiv Author ID - PubMed Author ID - Open ID respectively.

Indicate the contact for correspondence to the Author (Mail and Telephone) and indicate the Researcher who contributes as the first Author of the Article.

Plagiarism Detection

All Articles will be tested by plagiarism software PLAGSCAN if a plagiarism level is detected Positive will not be sent to arbitration and will be rescinded of the reception of the Article notifying the Authors responsible, claiming that academic plagiarism is criminalized in the Penal Code.

Arbitration Process

All Articles will be evaluated by academic peers by the Double-Blind method, the Arbitration Approval is a requirement for the Editorial Board to make a final decision that will be final in all cases. MARVID® is a derivative brand of ECORFAN® specialized in providing the expert evaluators all of them with Doctorate degree and distinction of International Researchers in the respective Councils of Science and Technology the counterpart of CONAHCYT for the chapters of America-Europe-Asia- Africa and Oceania. The identification of the authorship should only appear on a first removable page, in order to ensure that the Arbitration process is anonymous and covers the following stages: Identification of the Research Journal with its author occupation rate - Identification of Authors and Coauthors - Detection of plagiarism PLAGSCAN - Review of Formats of Authorization and Originality-Allocation to the Editorial Board- Allocation of the pair of Expert Arbitrators-Notification of Arbitration -Declaration of observations to the Author-Verification of Article Modified for Editing-Publication.

Instructions for Scientific, Technological and Innovation Publication

Knowledge Area

The works must be unpublished and refer to topics of Electromagnetism, electrical distribution sources, electrical engineering innovation, signal amplification, electric motor design, material science in power plants, management and distribution of electrical energies and other topics related to Engineering and Technology.

Presentation of the content

As the first article we present, *Implementation of an energy management system based on the ISO 50001 standard in a hospital clinic*, by HERNÁNDEZ-RIVERA, Carmen Elizabeth, VIDAL-SANTO, Adrián, MORALES-MARTÍNEZ, Mariel and JASSO-HERNÁNDEZ, Alberto, with affiliation at the Universidad Veracruzana, as the next article we present, *Application of the disturb and observe algorithm together with a control system for the boost converter in photovoltaic applications*, by MÉNDEZ-DÍAZ, Juan Francisco, PERALTA-SÁNCHEZ, Edgar, BONILLA-BARRANCO, Héctor and HERNÁNDEZ-SÁNCHEZ, Daniel Eduardo, with adscription in the Universidad Popular Autónoma del Estado de Puebla and Instituto Politécnico Nacional, respectively, as next article we present, *Energy Efficiency of a stones and minerals breaker plant in Campeche State to comply with the process Sizing of the photovoltaic system for a house located in the Presa la Concepción subdivision in Santiago Cuautlalpan, State of Mexico*, by HERNÁNDEZ-GÓMEZ, Víctor Hugo, MORILLÓN-GÁLVEZ, David, OLVERA-GARCÍA, Omar and GUZMAN-TINAJERO, Pedro, from the Universidad Nacional Autónoma de México, as last article we present *Design of a bidirectional converter for charging/discharging a supercapacitor*, by GARZA-GONZÁLEZ, Williams, DURÁN-GÓMEZ, José Luis, LÓPEZ-FLORES, David Ricardo and SÁENZ-VALVERDE, David Alberto, with affiliation at the Tecnológico Nacional de México campus Chihuahua.

Content

Article	Page
Implementation of an energy management system based on the ISO 50001 standard in a hospital clinic HERNÁNDEZ-RIVERA, Carmen Elizabeth, VIDAL-SANTO, Adrián, MORALES-MARTÍNEZ, Mariel and JASSO-HERNÁNDEZ, Alberto <i>Universidad Veracruzana</i>	1-10
Application of the disturb and observe algorithm together with a control system for the boost converter in photovoltaic applications MÉNDEZ-DÍAZ, Juan Francisco, PERALTA-SÁNCHEZ, Edgar, BONILLA-BARRANCO, Héctor and HERNÁNDEZ-SÁNCHEZ, Daniel Eduardo <i>Universidad Popular Autónoma del Estado de Puebla</i> <i>Instituto Politécnico Nacional</i>	11-26
Sizing of the photovoltaic system for a house located in the Presa la Concepción subdivision in Santiago Cuautlalpan, State of Mexico HERNÁNDEZ-GÓMEZ, Víctor Hugo, MORILLÓN-GÁLVEZ, David, OLVERA-GARCÍA, Omar and GUZMAN-TINAJERO, Pedro <i>Universidad Nacional Autónoma de México</i>	27-30
Design of a bidirectional converter for charging/discharging a supercapacitor GARZA-GONZÁLEZ, Williams, DURÁN-GÓMEZ, José Luis, LÓPEZ-FLORES, David Ricardo and SÁENZ-VALVERDE, David Alberto <i>Tecnológico Nacional de México campus Chihuahua</i>	31-39

Implementation of an energy management system based on the ISO 50001 standard in a hospital clinic

Implementación de un sistema de gestión de la energía con base a la norma ISO 50001 en una clínica hospitalaria

HERNÁNDEZ-RIVERA, Carmen Elizabeth†*, VIDAL-SANTO, Adrián, MORALES-MARTÍNEZ, Mariel and JASSO-HERNÁNDEZ, Alberto

Universidad Veracruzana, Facultad de Ingeniería Mecánica y Ciencias Navales, Campus Veracruz, Veracruz, Mexico.

ID 1st Author: *Carmen Elizabeth, Hernández-Rivera* / CVU CONAHCYT ID: 1020739

ID 1st Co-author: *Adrián, Vidal-Santo* / ORC ID: 0000-0002-3133-4332, CVU CONAHCYT ID: 38268

ID 2nd Co-author: *Mariel, Morales-Martínez* / CVU CONAHCYT ID: 1160912

ID 3rd Co-author: *Alberto, Jasso-Hernández*

DOI: 10.35429/JEE.2023.18.7.1.10

Received January 10, 2023; Accepted June 30, 2023

Abstract

In this article, an investigation was developed in a clinic located in the municipality of Veracruz, Ver. Mexico, with the objective of implementing an Energy Management System based on the Mexican official standard NMX-J-SAA-50001-ANCE-IMNC-2019, which is consistent with the international standard ISO 50001. The study was conducted in 2020 using historical consumption data from previous years, due to the pandemic situation that developed in later years, which was atypical for this type of study. The results of the plan for the implementation of the EnMS showed that the energy source that generates the highest consumption and cost is electricity. Similarly, it was determined that the level of compliance with the standard is 38%, obtained from the diagnosis covering the Plan-Do-Check-Perform stages. Based on the energy performance indicators and the energy baseline, it was established that the most significant variables are consumption/days, where it was determined that there is a possibility of saving 15.85% in energy consumption.

Resumen

En el presente artículo, se desarrolló una investigación en una clínica localizada en el municipio de Veracruz, Ver. México, con el objetivo de implementar un Sistema de Gestión de Energía con base a la norma oficial mexicana NMX-J-SAA-50001-ANCE-IMNC-2019, la cual tiene concordancia con la norma internacional ISO 50001. El estudio fue realizado durante el año 2020 utilizando datos históricos de consumo de años previos al mismo, debido a la situación de pandemia que se desarrolló en años posteriores y que fueron atípicos para realizar este tipo de estudios. Los resultados del plan para la implementación del SGen mostraron que la fuente de energía que mayor consumo y costo genera es la energía eléctrica. De igual manera, se determinó que el nivel de conformidad con la norma es de un 38%, obtenido del diagnóstico que abarca las etapas de Planificar-Hacer-Verificar-Actuar. A partir de los indicadores de desempeño energético y de la línea de base energética, se estableció que las variables más significativas son las de consumo/días, donde se determinó que existe una posibilidad de ahorro del 15.85% en consumo energético.

Energy management system, Hospitals, PHVA

Sistema de gestión de energía, Hospitales, PHVA

Citation: HERNÁNDEZ-RIVERA, Carmen Elizabeth, VIDAL-SANTO, Adrián, MORALES-MARTÍNEZ, Mariel and JASSO-HERNÁNDEZ, Alberto. Implementation of an energy management system based on the ISO 50001 standard in a hospital clinic. Journal Electrical Engineering. 2023. 7-18:1-10.

* Correspondence to the author (E-mail: elizabethrvr@live.com.mx)

† Researcher contributing as first author.

Introduction

Richard et al (2017) mentions that energy is fundamental to an organization's operations, so it can represent a significant cost, regardless of its activity. However, in addition to economic costs, energy can impose environmental and social costs due to resource depletion and contribute to problems such as climate change.

For its part, the NMX-J-SAA-50001-ANCE-IMNC-2019 standard, when referring to energy, talks about the types of energy that can be used in equipment or in a process, such as electricity, fuels, steam, heat, compressed air, and other similar means, including the renewable type. Then, in Mexico, as indicated by Chatellier Lorentzen & McNeil (2019) non-residential buildings are the largest consumer of energy in the country presenting an electricity consumption of 66.9 TWh during 2017.

Table 1 shows the electric energy consumption rates by type of building. It should be noted that the final uses of electrical energy in non-residential buildings are mainly for air conditioning and lighting, while in the industry it is used in motors to drive different devices. The warm-humid region mentioned in the table includes the states of Veracruz, Tabasco, Campeche, Yucatan, Quintana Roo, Guerrero, Oaxaca, Chiapas, and Colima. The clinic analyzed in this study is located in the state of Veracruz. Table 1 also shows that the main energy consumers are supermarkets and hospitals.

Buildings	kWh/m ² -year
Hotels	281
Offices	199.7
Schools	98.2
Hospitals	393.4
Restaurants	336.3
Stores	229.3
Supermarkets	443.1
Cinemas	242.8

Table 1 Rates of electrical energy consumption used by building type in the warm humid region of the country
Source: adapted from Chatellier Lorentzen & McNeil (2019)

In particular, the energy impact of the health sector in Mexico, recorded an energy consumption of 16.8 million MWh in electrical energy, 18.9 million MWh in fossil energy and the emission of 12.7 million tons of CO₂ per year, according to data from the Ministry of Energy (SENER, 2015), registering Veracruz as the state with the third highest energy cost, preceded by Mexico City and Puebla, as can be seen in figure 1.

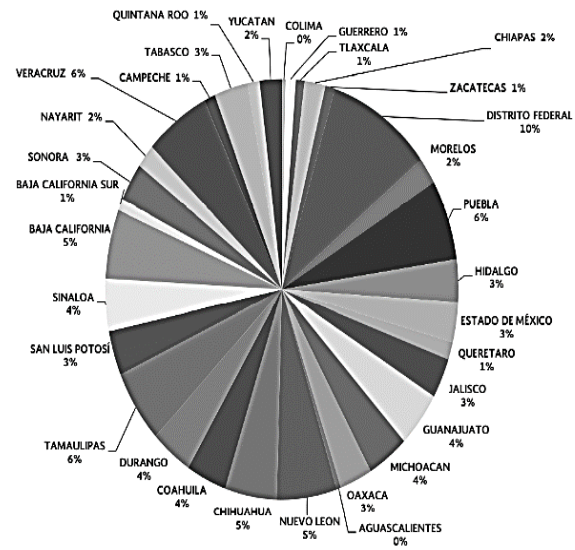


Figure 1 Energy cost in Health Care Units by state
Source: SENER (2015)

Therefore, it is recommended to take actions that improve energy efficiency and provide quick benefits to an organization, such as maximizing the use of its energy sources, which reduces both its cost and consumption, while positively contributing to the reduction of energy resource depletion and the mitigation of the effects of energy use worldwide, such as global warming ISO 50001 is based on the management system model and is the most widely used standard in the world. Jiménez Borges et al. (2018) mentions that more than eighty countries have adopted it as a national standard, given that ISO is the International Organization for Standardization and offers practical tools for the three dimensions of sustainable development: economic, environmental, and social.

The purpose of this standard is to enable organizations to establish systems and processes necessary to improve energy performance, including energy efficiency, use, and consumption. In order to reduce greenhouse gas emissions, energy costs, and other related environmental impacts, through systematic energy management (ISO, 2011).

Mexico has achieved the reduction of energy intensity thanks to the implementation of Mexican Official Standards (NOM) that came into force in the mid-1990s (De Buen Rodríguez, et al. , 2017). The present work is based on the NOM NMX-J-SAA-50001-ANCE-IMNC-2019, which is consistent with the International Standard ISO 50001, *Energy management systems - Requiriments with guidance for use*, ed2.0 (2018-08).

The Mexican standard defines a management system as a set of elements of an organization that interact to establish policies and processes to achieve objectives, taking into account the organization's structure, planning and operations.

Therefore, an Energy Management System (EnMS) is a system for establishing an energy policy, action plans, and processes to achieve energy objectives and targets. It uses interrelated elements such as Energy Performance Indicators (EPIs) and Energy Baselines (EBCs) to demonstrate measurable improvements in energy efficiency.

Energy efficiency is making the best use of available resources. It is the ratio or quantitative relationship between an output and an energy input. It is determined by factors such as:

1. Energy culture, which corresponds to the level of information existing in the organization and company policy.
2. The maintenance of equipment to achieve optimum yields.
3. Energy control, which involves measurement methods and the implementation of appropriate administrative processes.
4. Technological innovation or updating of technical resources.

De Buen Rodríguez (2020) indicates that the two basic actions for energy efficiency are: the modification of habits or best practices, which consist of using equipment when needed and in accordance with the need for energy service; and the replacement of technology with more efficient equipment.

Therefore, the efficient use of energy must obey a programmed process with the participation of all the organization's personnel. The successful implementation of an EnMS depends on the commitment of all levels of the organization, especially senior management.

The EnMS described in this standard is based on the plan-do-check-perform (PDCP) continuous improvement framework and is incorporated into existing organizational practices.

Methodology

This section presents the diagnostic analysis of the clinic by means of proposed questionnaires that evaluate its compliance, starting with the general definition of each component of the PDCA continuous improvement framework.

Energy performance indicators (EnPI)

To carry out each of the phases, we worked directly with the clinic director, administration, and maintenance personnel; in accordance with the standard of involving senior management in the continuous improvement process, surveys were conducted on the following points:

Planning

- Preliminary activity: Initial diagnostic analysis.
- Organizational context: Determine external and internal factors affecting energy performance.
- Leadership: Communicate to staff about the implementation of the EnMS.
- Planning: Identify activities that affect energy performance, set energy goals and objectives, identify energy types, evaluate energy use and consumption, identify USE, identify EPIs and EBCs, identify opportunities for improvement and document.

To do

- Support: Train personnel on EnMS, document training processes.
- Operation: Establish equipment operation criteria and communicate them to relevant personnel, take into account design and installation improvement opportunities, and document the operation process.

Checking

Performance evaluation: Verify that the USEs determine energy performance, implement energy performance monitoring and analysis methods, document information generated, and plan an audit program.

Performing

Improvement: Investigate causes and correct nonconformities, review by top management, record and document information generated.

In accordance with the above, the following results were obtained.

For the Planning phase of the organization's context section, it was determined that 86% of what is established in the standard is fully complied with, in leadership with 84%, and for planning, the results were similar, with 34% total compliance, 33% partial compliance, and 33% non-compliance.

In the To do phase, regarding support, a total compliance of 33% was established and 60% for partial compliance; and for operation, only 12% compliance and 63% partial compliance were determined.

For the Checking phase, with respect to performance evaluation, only 8% is complied with, while 46% is partially complied with.

Finally, in the Act phase, in the area of improvement, considering that the clinic had not implemented an EnMS before, there is no methodology to identify and correct nonconformities, so 80% do not comply, while the remaining 20% comply partially.

Results

In general terms, a summary of compliance and non-compliance with the standard can be seen in the diagram shown in Figure 2 below.

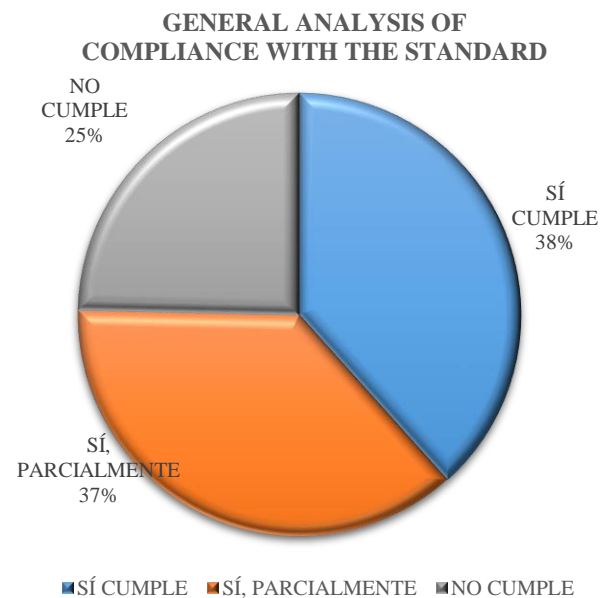


Figure 2 Results of the diagnostic analysis of the standard in the clinic

Source: Own elaboration

Attention to nonconformities in the EnMS.

Based on the results of the surveys, we proceeded to address the nonconformities of the standard, for which a schedule of activities was established. It should be noted that the standard is flexible during the execution of the PHVA cycle, so it allows modifying or improving the activities to be carried out depending on the importance given by the organization to the execution of the plan.

The activities to be incorporated in the organization to comply with the schedule are described below.

Planning

It is important to identify factors that influence the context of the organization, such as financial, legal, social, external and internal factors. In terms of leadership, it is necessary to incorporate the topic of energy savings in conversations and in the decision-making process with management staff, in order to integrate the EnMS into the organization's philosophy. Otherwise, the EnMS would only remain at a documentary level without being applied in daily work practices.

For the planning section, it is first necessary to perform an energy performance assessment. For this, Flores Díaz et al. (2016) indicate that organizations should identify legal requirements and those that are linked to energy use, consumption and efficiency. For the detection of energy performance improvement opportunities, energy consumption and use data were collected, including relevant variables. Also, energy sources were identified, including diesel fuel, LP gas and electricity. Figures 3 and 4 show the forms of utilization and storage for the first two mentioned above.



Figure 3 Emergency electric generator of the clinic, operated with diesel

Source: Own elaboration



Figure 4 Clinic's stationary LP gas tank for restaurant and laundry use

Source: Own elaboration

Regarding electrical consumption, the distribution of the power (W) of connected loads is as follows: the greatest electrical demand corresponds to the central or package air conditioning systems with 31% of the clinic's total power; in second place are the X-ray area and the operating room area, both with 17%, while the administrative area corresponds to 8%.

Figure 5 shows a diagram of the costs generated by water and electricity consumption during 2019, due to the amount of information available and because, due to the pandemic situation in the following years, a decrease in the usual flow of work was generated.

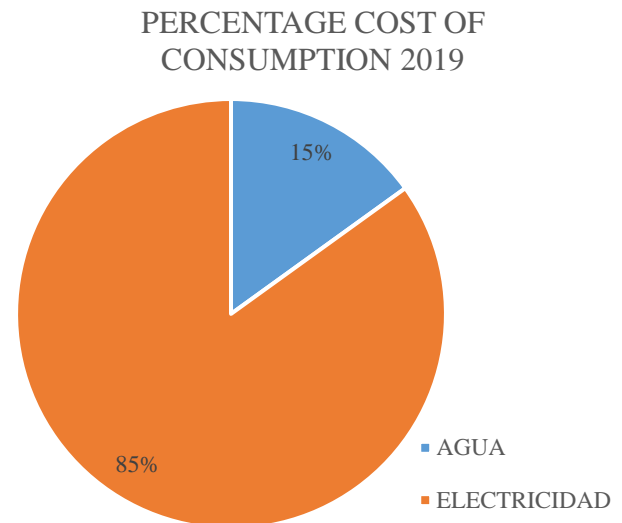


Figure 5 Percentage cost of energy sources in the clinic during 2019

Source: Own elaboration

Considering that the highest costs were for electricity consumption, it can be determined that the study to be carried out to implement the EnMS will be focused on the electrical area.

Based on the data obtained about the loads connected in the clinic, the USE (significant energy uses) can be determined. Central or package air conditioners (AAC) stand out with 9063.12 kWh/month, followed by mini splits with 3183.02 kWh/month and elevators with 2168.64 kWh/month. Table 2 shows the consumption of specific medical equipment.

EQUIPMENT	kWh/month
Fixed X-ray	267.86
Autoclave	121.71
Compressor	63.92
Oxygen plant	38.35
Electrocautery	30.17
Anesthesia machine	10.29
Yellow bulb RX	9.72
Ultrasound	9.72
Surgical Light	7.54
Ring light	5.76
Incubator	5.14
Ophthalmoscope/Otoscope	4.08
Negatoscope	1.48
Defibrillator	0.4
Stretchers light	0.35
Computerized radiography	0.2

Table 2 Medical equipment

Source: Own elaboration

Baseline

According to the ISO 50001 (2018), the energy baseline is defined as a "quantitative reference that provides the basis for comparison of energy performance."

According to the Technical Guide for the implementation of Energy Management Systems in the framework of a Learning Grid (Richard et al, 2017) the energy baseline can be represented by absolute energy consumption values or normalized consumption values by means of relevant variables (climate, production data). It can be the historical consumptions or the consumptions calculated considering that the organization would not have carried out actions to improve energy performance. A period appropriate to the use and consumption of energy in the organization must be considered.

The most common is to consider the cycle of the relevant variables defined in the energy performance diagnosis, generally 12 months, for climatological data or the company's production cycle. Some organizations change their energy baseline every year and usually measure the current year's results against those of the previous year. In this case, this practice should be documented. Do not forget that the energy baseline is established according to the scopes and limits defined for the EnMS, i.e., if the EnMS does not include all areas of the plant, the energy baseline cannot be the total energy consumption of the plant.

The energy baseline (EBCs) reflects a specific period of time as a reference point, in this case it was the consumption recorded in the invoices during 2019. While, the proposed energy performance indicators (EPIs) was: kWh/days, kWh/patient, kWh/temperature. Together, the EBCs and the EPIs will function as a tool for continuous monitoring of energy performance.

In table 3 the values and days of consumption were obtained from the invoices provided, the average monthly temperature for the state of Veracruz was consulted in METEORED and the number of patients was an estimated 1.5 patients attended per day at the clinic, the number of days billed was 1.5.

Month	Consumption [kWh]	Days	°C	Number of patients
January	8000	-	23	-
February	7200	31	23	46.5
March	9280	-	26	-
April	8160	28	29	42
May	13280	-	29	-
June	15360	32	29	48
July	14240	29	29	43.5
August	13600	-	28	-
September	16320	33	28	49.5
October	13920	30	27	45
November	11200	33	25	49.5
December	9760	29	22	43.5

Table 3 2019 data to determine EBCs and EPIs

Source: Own elaboration

The proposed NDIs are intended to analyze the relationship between consumption and the independent variables. It is important to mention that the EPIs can be changed, increased or deleted depending on the needs of the clinic and/or taking into account if there are other relevant factors that could arise in the course of the implementation of the EnMS.

In many cases, a simple linear relationship is adequate to determine the relationship between variables. The ISO 50006 (2014) explains that, in a scatter diagram, if the points appear to be scattered around the trend line, it is indicative of the presence of relevant variables. On the other hand, if the points appear as a random cloud with no obvious relationship, it is likely that the variable is not relevant.

For this case, the response variable was defined as consumption in kWh, and the independent variable as the days billed, number of patients and average ambient temperature. Lara Izaguirre et al. (2019) mentions that the coefficients of determination (R^2) indicate the proportion of variance of the variable y in relation to the independent variable x. Where if R^2 tends to zero, the model does not adequately represent the data. But if it tends to 1, the model adequately represents the data explained by the linear regression model.

For the first case, the consumption data were evaluated with respect to the days billed, as shown in figure 6.

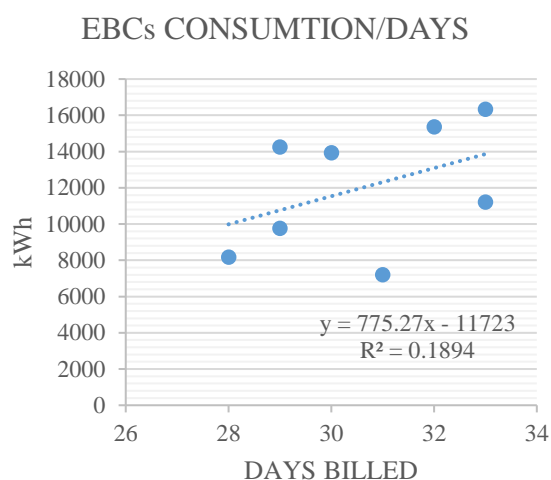


Figure 6 EBCs calculated with EPIs kWh/day
Source: Own elaboration

It was found that the variable days billed is not very significant for electricity consumption, based on the correlation coefficient R^2 of 0.1894. For it to be significant, the value should be in the range of 0.7 to 1.

Figure 7 shows the estimated target line for the same data.

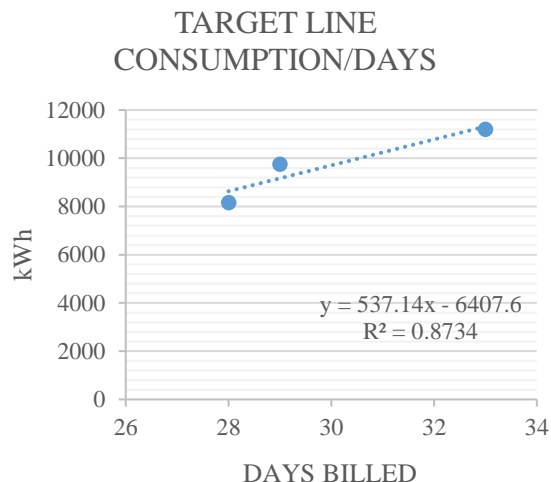


Figure 7 Estimated target line with EPIs kWh/day
Source: Own elaboration

From the baseline, the points of best performance were obtained, i.e., the months with the lowest billing (marked in bold in table 2), which would represent the efficiency that can be achieved in the clinic. The R^2 coefficient obtained based on these points is 0.8734, indicating that there is a valid relationship between consumption and days billed. It should be remembered that these calculations are only estimates, since they depend on the clinic's commitment to implement energy efficiency actions.

With the equations obtained from the EBCs and the target line, the monthly savings potential can be estimated, assuming that x is equal to 30 days:

Where the target line has the equation:

$$y = 537.14x - 6407.6 \quad (1)$$

$$y = 9706.6$$

And where the EBCs has for equation:

$$y = 775.27x - 11723 \quad (2)$$

$$y = 11535.1$$

The electrical consumption saving (ECS) would be:

$$ECS = 11535.1 - 9706.6$$

therefore:

$$ECS = 1828.5 \text{ kWh/month}$$

which corresponds to 15.85%.

Performing the same analysis with the kWh/patient and kWh/temperature EPIs to continue with the evaluation of the relationship between consumption and the independent variables, it was observed that the correlation coefficient in all cases was less than 0.7, which established that they were not relevant indicators for the study. In the case of consumption/patient, it is recommended that a record be kept of the number of patients attended in order to estimate a more significant relationship. Although the R^2 coefficient is low for the aforementioned indicators, it should be noted that the behavior of the line is due to the fact that the highest consumption was due to both the number of patients attended and the average temperature in November, followed by December, which had a higher number of patients compared to April, despite having a low average temperature of 22°C, as shown in table 3.

Based on the analyzed, energy goals and objectives were proposed as energy goals and objectives to reduce energy consumption by at least 15%, corresponding to 1730.4 kWh/month, such amount is equivalent to 1.007 Ton of CO₂ eq/MWh that would no longer be emitted to the atmosphere, applying the factor 0.582 Ton of CO₂/MWh of Emission of the National Electric Sector of 2017, whose value updated to 2021 is 731.9592 Ton of CO₂ eq/MWh using a factor of 0.423, reported by the Energy Regulatory Commission (CRE, 2021).

At the same time, the measures proposed to be implemented are as follows:

- Disconnect equipment at the end of working hours to avoid "vampire" consumption.
- Turn off lights in areas that are not in operation.
- During the day, take advantage of natural light and do not turn on lights (depending on the work area, such as offices and consulting rooms).
- Close the doors of unoccupied facilities to reduce the strain on the air conditioners.
- Replace window air conditioners with mini splits.
- Replace light bulbs with LED bulbs in facilities under renovation.
- Reduce consumption of air conditioners during cold seasons.
- Post signs to remind important aspects of the operation of the facilities and allow energy savings ("Remember to turn off the light when leaving", "Disconnect your computer before leaving", etc.).
- Keep a weekly record (at most) of the meter to visualize the progress of the system.

To do

In terms of support, it is recommended to differentiate the profile of people and create a training program accordingly, so that everyone has general knowledge about the concepts of energy, energy efficiency, USE, etc., but only personnel in specific areas such as the operating room and X-ray, have access to information on maintenance and operation of their work equipment for efficient management that does not compromise their safety. This is because the staff influences the energy performance of the clinic, therefore, they need to be competent and aware of the impact they have on the operation of the EnMS. Regarding operation, it is important to determine the operational control criteria and maintenance criteria. These criteria serve to identify activities that affect equipment performance. However, they can also be applied for the design of new facilities, or for modifications of equipment, systems and processes that have an impact on energy performance. For these cases, internal communication between energy procurement personnel (in the case of implementing renewable energy sources) and those who manage energy performance activities must take place in order to prevent and control risks.

Checking

To verify, in terms of performance evaluation, it is known that a continuous evaluation system allows for the timely identification of the actions necessary to ensure compliance with energy objectives and goals. In this case, it was proposed to reduce monthly electricity consumption, so weekly monitoring is recommended to observe whether energy deviations are generated. In order to review the effectiveness of the EnMS, it is necessary to implement an internal audit process. Once the audit has been carried out, corrective and preventive actions must be implemented.

Performing

In the area of improvement, the review by top management should take place shortly after completion of the energy performance assessment together with the inventory of opportunities for improvement, or until after the internal audit has been performed.

The results of this review should be: recommendations for the new expected energy consumption (for the next period), changes in the EnMS, updates in the energy policy and in the established objectives.

This is due to the fact that an EnMS is permanent, so the continuous improvement of the process and its design and implementation activities must be guaranteed.

Acknowledgments

To CONAHCYT for the National scholarships granted to the students Carmen Elizabeth, Hernández Rivera, and Mariel Morales Martínez of the master's degree in Applied Engineering-PNPC of the Universidad Veracruzana.

Conclusion

In Mexico, non-residential buildings such as supermarkets and hospitals are the main energy consumers. Therefore, implementing an energy management system (EnMS) in a health care unit helps to mitigate the problem with greenhouse gases and save resources, both energy and economic.

In the case study, electricity was identified as the main source of consumption, as well as the USE determined by central air conditioners, mini splits, elevators and computer equipment. The EPIs as energy consumption in kWh per month evaluated by days billed, temperature and average number of patients attended, which allowed determining EBCs during 2019 and proposing an energy target line. A 15.85% savings in energy consumption was calculated, which can be achieved as long as senior management remains committed and energy efficiency measures are implemented, as well as communication with the clinic staff to ensure the success of the EnMS.

If the observations are taken into account, as well as the implementation of the proposed recommendations, the clinic can be re-evaluated to identify the new level of compliance with the standard, with the expectation of exceeding the 38% obtained in the initial diagnosis. If a high percentage is obtained and if it is the clinic's wish, an internal audit could be carried out in order to obtain an official ISO 50001 certification.

References

Richard, N., Ortigosa, J., Liliana Caballero, S., Córdova, A. D., & Feilbogen, E. (2017). Guía técnica para la implementación de Sistemas de Gestión de la Energía en el marco de una Red de Aprendizaje. Ciudad de México. Obtenido de https://energypedia.info/images/d/d2/Guia_tecnica_Participante_2017.pdf

Chatellier Lorentzen, D., & McNeil, M. (2019). Consumo de electricidad de edificios no residenciales en México: La importancia del sector de servicios. CONUE. From https://www.conuee.gob.mx/transparencia/boletines/Cuadernos/cuaderno3nvciclo_2.pdf

SENER. (2015). Estudios en materia de eficiencia energética. Gob.mx. From https://www.gob.mx/cms/uploads/attachment/file/315521/2_HOSPITALES.pdf

Jiménez Borges, R., Monteagudo Yanes, J. P., Wilson, H., & García Reyes, D. R. (2018). Análisis del Sistema Energético de un hospital basado en la norma NC ISO 50 001 [Presentación de diapositivas]. IV Evento Nacional de Experiencias en Sistemas Integrados de Gestión. Centro de Estudios de Energía y Medio Ambiente Universidad Cienfuegos. From https://www.researchgate.net/publication/323756016_Analisis_del_sistema_energetico_de_un_hospital_basado_en_la_norma_NC_ISO_50_001

ISO. (2011). Gana el desafío de la energía con ISO 50001. Traducción realizada por COPANT bajo su responsabilidad, con la autorización de ISO. From <https://docplayer.es/1624926-Gana-el-desafio-de-la-energia-con-iso-50001-iso-50001-gestion-de-la-energia.html>

De Buen Rodríguez, O. D., Navarrete Barbosa, J. I., Jáuregui Nares, I., Hernández López, P., Chávez Sandoval, F. d., & García Rodríguez, H. F. (2017). Hoja de Ruta en Materia de Eficiencia Energética. Ciudad de México: CONUE. From https://www.gob.mx/cms/uploads/attachment/file/313765/HojadeRutadeEficienciaEnergeticavOdeB24012017SCC_07112017_VF.pdf

DOF. (2018). Norma Mexicana NMX-J-SSA-50001-ANCE-IMNC-2019. Sistemas de gestión de la energía-Requisitos con orientación para su uso (cancela a la NMX-J-SAA-50001-ANCE-IMNC-2011). From https://www.dof.gob.mx/nota_detalle.php?codigo=5585826&fecha=07/02/2020

De Buen Rodríguez, O. (2020, agosto). Beneficios de los Sistemas de Gestión de la Energía ISO- 50001. [Presentación de diapositivas] From https://www.gob.mx/cms/uploads/attachment/file/582857/Beneficios_de_SGEN-AGO-2020.pdf

Flores Díaz, L., Escobosa Pineda, N., Espinosa Flores, L. (2016, julio). Manual para la Implementación de un Sistema de Gestión de la Energía. 2da Edición. CONUEE / GIZ. From https://www.gob.mx/cms/uploads/attachment/file/119159/Manual_SGen_Conuee_2da_Edicion.compressed.pdf

ISO. (2018). ISO 50001:2018 Energy management systems — Requirements with guidance for use. From <https://www.iso.org/standard/69426.html>

ISO. (2014). ISO 50006:2014 Energy management systems — Measuring energy performance using energy baselines (EnB) and energy performance indicators (EnPI) — General principles and guidance. From <https://www.iso.org/standard/51869.html>

Lara Izaguirre, B. I., Acosta Pintor, D. C., Ramírez Aguilar, C., Vidal Becerra, E. (2019, septiembre). LÍNEA DE BASE ENERGÉTICA: ESTUDIO EN HOSPITAL PÚBLICO. Tectzapic. Vol 5(2). From <https://www.eumed.net/rev/tectzapic/2019/02/base-energetica.html>

CRE (2021). Factor de Emisión del Sector Eléctrico Nacional. Gob.mx. From https://www.gob.mx/cms/uploads/attachment/file/706809/aviso_fesen_2021.pdf

Application of the disturb and observe algorithm together with a control system for the boost converter in photovoltaic applications

Aplicación del algoritmo perturbar y observar junto con un sistema de control para el convertidor elevador-boost en aplicaciones fotovoltaica

MÉNDEZ-DÍAZ, Juan Francisco^{†*}, PERALTA-SÁNCHEZ, Edgar^{''}, BONILLA-BARRANCO, Hector^{'''} and HERNÁNDEZ-SÁNCHEZ, Daniel Eduardo^{'''}

^{*} Facultad de Ingeniería Ambiental, Centro de Investigación en Potencia Eléctrica y Energías Limpias. Universidad Popular Autónoma del Estado de Puebla. Puebla, México.

^{''} Centro de Investigación en Potencia Eléctrica y Energías Limpias. Universidad Popular Autónoma del Estado de Puebla. Puebla, México.

^{'''} Centro de Investigación en Potencia Eléctrica y Energías Limpias. Universidad Popular Autónoma del Estado de Puebla, Centro de Innovación y Desarrollo Tecnológico en computo, Instituto Politécnico Nacional. Puebla, México.

ID 1st Author: Juan Francisco, Méndez-Díaz / ORC ID: 0000-0001-6267-3671, CVU CONAHCYT ID: 292499

ID 1st Co-author: Edgar, Peralta-Sánchez / ORC ID: 0000-0001-2602-5025, CVU CONAHCYT ID: 40745

ID 2nd Co-author: Héctor, Bonilla-Barranco / ORC ID: 0000-0002-5020-7312, CVU CONAHCYT ID: 553622

ID 3rd Co-author: Daniel Eduardo, Hernández-Sánchez / ORC ID: 0009-0003-5527-8587, CVU CONAHCYT ID: 700596

DOI: 10.35429/JEE.2023.18.7.11.26

Received January 15, 2023; Accepted June 30, 2023

Abstract

The boost-boost converter presents interesting characteristics for photovoltaic applications, due to the nature of the system where we can increase the voltage in an adequate and controlled way according to the load, in combination with an optimal control system we can obtain a better efficiency of an autonomous photovoltaic system, taking into consideration that a solar panel within its most significant properties to operate within the most efficient way needs natural conditions of irradiation and temperature that are closest to the SCT measurement standard, otherwise efficiency will be lost. Therefore, it is necessary to jointly implement a control system together with an algorithm that allows it to always be in maximum power conditions (MPP). According to the above, this article addresses the low voltage photovoltaic application of an isolated system, using a boost converter and a PI control system, together with an algorithm for obtaining the maximum power point, using two different photovoltaic systems, with the objective of showing that with an essential PI control we can obtain good efficiency of the two systems even with disturbances, as if a more robust control were implemented in photovoltaic applications, saving both operation cost and implementation time. The I-V (current-voltage) characteristics similar to a non-linear source of the photovoltaic module, require the inclusion of linearization of the photovoltaic module and with this to be able to design the control of the system, the proper functioning of the designed control has been tested through mathematical modeling and simulation.

DC/DC converters, Autonomous photovoltaic systems, Control systems, MPPT perturb and observe, Energy efficiency

Resumen

El convertidor elevador-boost presenta características interesantes para aplicaciones fotovoltaicas debido a la naturaleza del sistema, por ejemplo, es posible aumentar el voltaje de una manera adecuada y controlada de acuerdo con la carga. En combinación con un sistema de control óptimo podemos obtener una mejor eficiencia de un sistema fotovoltaico autónomo, teniendo en consideración que un panel solar dentro de sus propiedades más significativas para operar dentro de manera más eficiente necesita de condiciones naturales de irradiación y temperatura lo más cercanas al estándar de medida SCT, de no ser así se perderá eficiencia, por lo que es necesario implementar de manera conjunta un sistema de control con un algoritmo que le permita siempre estar en la condiciones de máxima potencia (MPP). De acuerdo con lo anterior, en este artículo se aborda la aplicación fotovoltaica en bajo voltaje de un sistema aislado, utilizando un convertidor elevador-boost, un sistema de control PI y un algoritmo de obtención del punto de máxima potencia. Se utilizan dos sistemas fotovoltaicos diferentes con el objetivo de mostrar que con un control PI esencial podemos obtener buena eficiencia de los ambos sistemas aun con presencia de perturbaciones al igual que si se implementara un control más robusto en aplicaciones fotovoltaicas permitiendo un ahorro tanto de costo de operación como de tiempo en la implementación. Las características I-V (corriente-tensión) similar a una fuente no lineal del módulo fotovoltaico requieren la inclusión de linealización del módulo fotovoltaico y con esto poder diseñar el control del sistema. El funcionamiento del control diseñado ha sido probado mediante el modelado matemático y por simulación.

Convertidores conmutados DC/DC, Sistemas fotovoltaicos autónomos, Sistemas de control, MPPT perturbar y observar, Eficiencia energética

Citation: MÉNDEZ-DÍAZ, Juan Francisco, PERALTA-SÁNCHEZ, Edgar, BONILLA-BARRANCO, Héctor and HERNÁNDEZ-SÁNCHEZ, Daniel Eduardo. Application of the disturb and observe algorithm together with a control system for the boost converter in photovoltaic applications. Journal Electrical Engineering, 2023. 7-18:11-26.

* Correspondence to Author (E-mail: juanfransisco.mendez@upaep.mx)

† Researcher contributing as first author.

Introduction

In recent years the demand for energy has increased continuously, with the main source being the indiscriminate use of fossil fuels. This constantly growing energy demand has generated an increase in greenhouse gases, causing severe damage to the environment, such as global warming and the worldwide problem of climate change. Thus, in the global energy context, renewable energies have emerged as a response to the social demand to reduce CO₂ emissions and other pollutants of direct action.

Photovoltaic systems are one of the most studied models for obtaining electricity from renewable sources. According to (Ram, et al., 2017), a particularity when using photovoltaic systems for energy production is the fact that the electrical voltage generated by the photovoltaic panels, which has a non-linear relationship with irradiation, so that the maximum voltage generated does not represent the maximum power that the panel can deliver to an electrical load. Given this non-linearity, the maximum power that the PV panel can deliver is a function of the combination of voltage and current in the electrical load.

This non-linearity presented by the solar panels tries to be solved by determining an operating point or maximum power point (MPP) as long as it is at standard measurement conditions (STC). According to the literature, the STC of the solar panel should be at a temperature of 25°C and an irradiation of 1000 W/m² on the surface of the panel. The performance of the most promising PV technology should be regulated according to the MPP. The output of the PV system is affected by temperature, irradiation and partial shading. These changes in environmental conditions limit the efficiency and power output of the panel and the measured output of the panel deviates from the desired set point. To improve the MPP there is the Maximum Power Point Tracker (MPPT) as it estimates and controls the MPP. The design of the MPPT system to achieve a regulated output is done using voltage converters and controllers to converge the MPP even under distribution conditions. There are different types of converters and controllers to optimise the efficiency of the PV panel using MPPT (Sharma & Jain, 2015).

As mentioned before, one of the most important parts to obtain higher efficiency of PV systems is the implementation of algorithms to always find the maximum power point in combination with various control strategies (MPPT: MPP tracking). There are several algorithms, among the most used according to the scientific literature are: the Perturb and Observe method, Incremental Conductance, the Constant Voltage method and the Fuzzy Logic method. In this article, each of them will be explained in general terms, except for the Disturb and Observe algorithm, which is the one used in this work and will be explained in more detail.

According to (Ebrahimi & Viki, 2015), DC-DC converters are widely used in renewable energy generation systems such as solar photovoltaic systems, wind systems and in fuel cells, this in order to obtain a correct energy conversion, as shown in figure (1). A solar photovoltaic (PV) power generation system is used in grid-connected applications and in stand-alone or islanded system, where to improve its efficiency, switched converters can also be implemented (Saravanan & Ramesh Babu, 2017). In (Alam & Hoque, 2019) it is proposed that the most suitable power converter to solve the problem of low voltage levels obtained from PV panels is the boost-boost converter; which raises and regulates the output voltage. The input of the boost converter acts as a current source due to the input inductor, which means that it has almost constant input current, which is favourable in PV systems. By interleaving the boost converters, low ripple current is achieved in the input current, output voltage and high power conversion. This topology can be used for the interface connection between the low voltage of the PV array and a high input voltage of the battery bank or any DC load (Taghvaei, *et al.*, 2013).

The boost converter helps to increase the voltage level, improve stability and power factor. In some cases, the converter can also be used as a pre-regulator. It is clear that DC-DC converters require an acceptable and efficient operation for the PV system to be effective and have the least possible energy losses, this also depends directly on the control that is used in the system and ensures the smooth operation of the system even in the presence of disturbances.

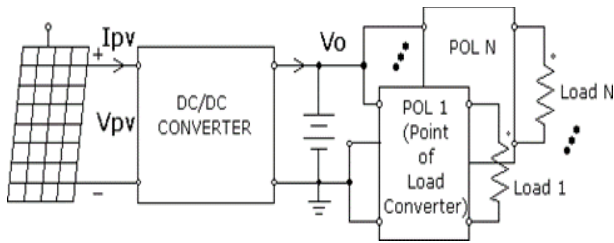


Figure 1 Photovoltaic system architecture with serial DC bus

Source: Méndez *et al.*, 2014

Another application of boost-boost converter is proposed in (Dhople *et al.*, 2009), where three boost converters are interleaved in which they found superior current characteristics compared to the coupled converters. In (Tian *et al.*, 2016), they use an improved interleaved boost circuit, concluding that this is the most suitable for photovoltaics using an MPPT algorithm, as it has greater advantages than the traditional interleaved boost converter (TIBC) and the single boost converter (SBC) such as:

Higher tuning ratio

More stable, accurate output voltage with less ripple.

Lower switch voltages

It is useful for increasing system efficiency and reducing energy losses.

According to the above, in order for the operating system to function properly, a control model needs to be developed to enable proper operation. Among the control systems for photovoltaic applications with switched DC/DC converters are Proportional Integral Derivative (PID) and Proportional Integral (PI). According to (Dwivedi & Saket, 2017), in PV system the value of maximum power, current and peak voltage are increased by controlling the gain of PID controller. In (Rabiaa *et al.*, 2019) a cascaded closed-loop control using PI controller is proposed for DC-DC boost converter showing good performance in terms of rise time, disturbance rejection and steady state error.

Furthermore, it is shown that the DC-DC boost converter has a strongly non-linear dynamic behavior, so the performance of any linear controller such as the PI controller can only be optimal as long as the system remains around a certain operating point, i.e. for photovoltaic applications where solar panels are characterized by their non-linear structure, and if a PI or PID control is to be applied, which are controls characterized by using linearized models around an equilibrium point, the behavior of the solar panels must be linearized by means of their basic equation. If this were not the case and it is desired to work with the non-linear structure, other control modes would have to be used, such as the sliding mode control used in (Méndez, *et al.*, 2014; Méndez, *et al.*, 2015; Méndez, 2018 and Méndez, *et al.*, 2019).

Therefore, this article presents the analysis of the boost converter used in two different photovoltaic systems to carry out a comparison between them, implementing a PI control system, with the aim of showing that with an essential control as this widely used in various systems, we can obtain an optimal control performance in the event that disturbances occur, as if it were to implement a more robust control, reducing costs and operating times. Also, to make the system more efficient in combination with PI control, the MPPT Perturb and Observe algorithm is implemented, which helps the PV to operate more efficiently, as it always looks for the point of maximum power. In our application we can obtain the control of the input voltage V_{PV} of two different PV panels. Considering the parasitic losses that are present in a real system, together with the representative non-linearity of the PV panels. For this reason, the models of both panels are linearized to work around an equilibrium point, to obtain the MPPT even when presenting disturbances, obtaining as a result an optimal response in both systems. The analysis is performed with two different panels with powers of 85 W and 100 W. For the 85 W panel, the article (Méndez *et al.*, 2015) was taken as a reference, where the same panel is used.

The objective of this work can be listed as follows:

To present a general approach to derive the transfer function of the boost-boost DC-DC converter and achieve system control on both solar panels.

Present a PI controller design approach for the input voltage of the PV panels to achieve a constant output voltage independent of the load variation.

Present the implementation of the controller using mathematical modelling and the control system to verify the results of each design.

Demonstrate that with a control such as the PI control, satisfactory results can be obtained in two types of solar panels with different powers, and that these respond appropriately in the event of disturbances in the system.

To implement together with the PI control an MPPT Disturb and Observe algorithm to make the system more efficient.

Theoretical analysis

Boost-Boost Converter

The circuit diagram of the boost converter, as shown in figure (2), consists of an electronic switch which is controlled by a pulse width modulation (PWM) signal. The inductor stores the energy coming from the source until the T_{on} period when the electronic switch is turned on. Meanwhile, when the diode is reverse biased, it isolates the output of the circuit and the load current is supplied from the capacitor (Méndez, *et al.*, 2014). When the electronic switch is off, the inductor is discharged and current flows through the diode. The output voltage is composed of the discharged voltage and the instantaneous panel voltage, so it is always higher than the input voltage. The switch on and off is controlled by the PWM signal (Bouchakour *et al.*, 2015).

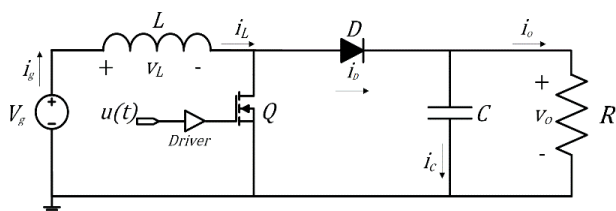


Figure 2 Schematic of the boost converter
Source: Méndez, 2018

Therefore, for the research presented in this paper, one of the elementary converters, the boost converter, is used in combination with the solar panel and a battery, which will have a linear behavior as shown in figure (3) and a PI type control is applied together with the MPPT Disturb and Observe algorithm.

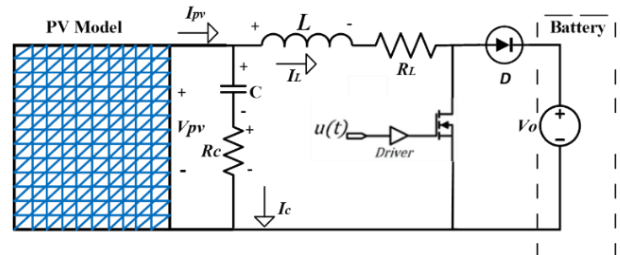


Figure 3 Performance of a solar panel and battery with a boost converter

Source: Own elaboration

Analysis of the Photovoltaic Panel, and Maximum Power Point (MPPT)

As expressed in (Leuchter, *et al.*, 2012), photovoltaic panels are non-linear systems, because there is a yield loss that is distributed non-linearly and parametrically (with solar irradiance and temperature) along the panel voltage axis, i.e. the direct application of Shockley's equation, $I = I_0 * \left[e^{\frac{v}{n * V_t}} - 1 \right]$, good modelling results are not available for any panel, and the main reason is the existence of power losses which extend along the voltage axis in a non-linear way.

In addition to these facts, the quality of the semiconductor material n is also variable and depends on the manufacturing process and the semiconductor material. Other aspects that affect the efficiency of the system are solar radiation and temperature, so when connecting to a DC/DC converter, it is first necessary to linearize the PV panel and then to linearize the converter. The technique for linearizing the converter in this article is performed using state space analysis. For the analysis of the PV systems, we use the parameters from the specification sheets of each PV system, and the classical simplified model of the i - v relationship of the PV module as shown in figure (4) (Méndez, *et al.*, 2015).

Figure (4) also shows the maximum power point, with the temperature and irradiation factor and the power factor, which as we can see depends directly on external factors such as existing weather changes.

Due to the above, MPPT algorithms must be constantly improved to be more effective and accurate so that external changes to the panel do not significantly affect it (Méndez, *et al.*, 2014; Méndez, *et al.*, 2015; Méndez, 2018 and Méndez, *et al.*, 2019).

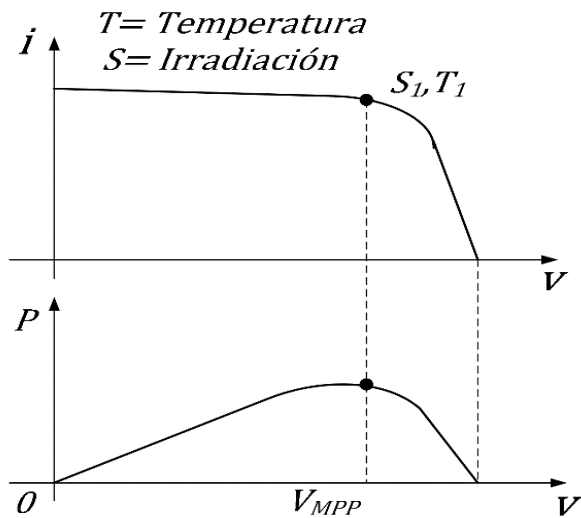


Figure 4 Maximum Power Point

Source: Méndez, 2018

As mentioned above, photovoltaic panels must work at maximum power point, for this, several systems and techniques must be related to take advantage of the maximum energy that can be produced, this adaptation must have certain particularities such as: good performance, feasibility, and a dynamic and balanced behavior. As an example of this, figure (5) shows the solar panel in operation, the sensors for measuring both voltage and current, and the integration of the MPPT algorithm together with the direct connection to the converter, and from the converter to the load, which in this case is a battery that has a linear behavior.

With this we begin to guarantee the obtaining of maximum power, where only the control technique is missing, which will help to achieve greater precision and ensure considerable energy production, even if there are sudden changes in temperature, this will be translated as existing disturbances in the system, so the PI controller will have to operate efficiently for optimal work of the PV (Méndez, *et al.*, 2014; Méndez, *et al.*, 2015; Méndez, 2018 and Méndez, *et al.*, 2019).

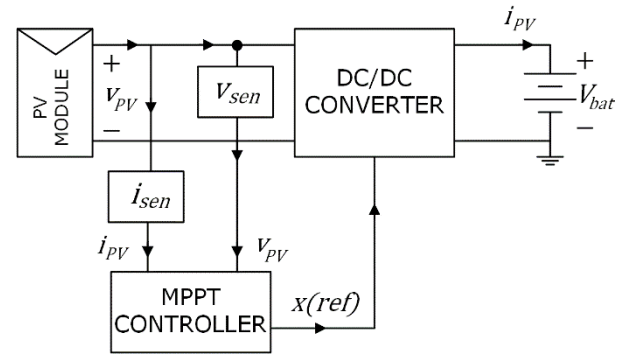


Figure 5 Switched-mode converter with MPPT

Source: Méndez, 2018

Disturb and Observe algorithm and algorithms for obtaining the Maximum Power Point (MPPT)

- As presented, obtaining the maximum power point MPPT plays a relevant role in the efficiency of solar panels, and therefore, the development of MPPT algorithms becomes paramount.
- One of the most widely used algorithms in the literature is the incremental conductance algorithm. This method is based on the fact that the slope of the power curve versus the voltage generated by the solar panel is zero at the MPP maximum power point, i.e. the maximum power point can be traced by comparing the instantaneous conductance I/V with the incremental conductance $\Delta I/\Delta V$. Among its advantages is its good dynamic response to rapidly changing atmospheric conditions. Its main disadvantage is a higher complexity in the creation of the algorithms compared to other methods. Another algorithm mentioned in the literature is the constant voltage tracking (CVT), this method is based on the intensity of light reflected on the solar panel, when this light intensity is present, the temperature of the panel also changes. At that moment the system measures the voltage produced from the illumination and temperature, and with this it calculates the MPP, and makes it work close to it. This method presents simple, convenient and feasible solutions, but has a disadvantage that it does not operate properly when sudden temperature changes occur.

Another algorithm that is more widely used and is the one employed in this work is the Disturb and Observe algorithm. As shown in figure (6), we have the flow chart of the algorithm which shows the principle of this method based on modifying (perturbing) the operating voltage of the PV array in a certain direction. If the extracted power is increased, it means that the operating point has moved towards the MPP, therefore, the operating voltage should continue to be perturbed in the same direction. If, on the other hand, the power obtained after the perturbation is reduced, it is assumed that the system is moving away from the MPP and the direction of the voltage perturbations must be reversed. The main advantage of this method is that it is easy to implement. Its disadvantage is that the system never operates exactly at the MPP but oscillates around it and the power generated is lower than the theoretical maximum (Méndez, *et al.*, 2014; Méndez, *et al.*, 2015; Méndez, 2018 and Méndez, *et al.*, 2019).

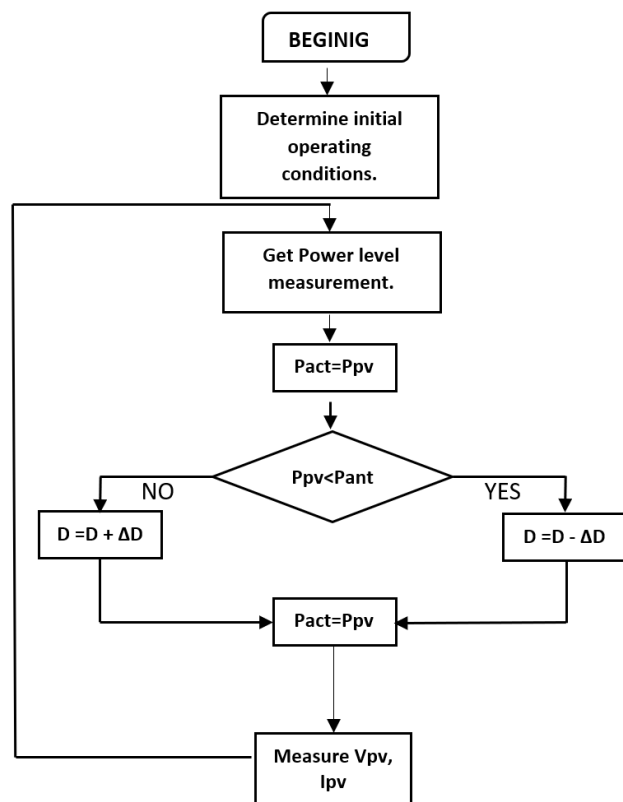


Figure 6 Maximum Power Point Algorithm
Source: Own elaboration

Solar Panel Linearisation

According to the above, we see the importance of having a good MPPT algorithm interacting with the various systems involved in a PV, but for the mathematical analysis we must linearize the behaviour of our photovoltaic panel as shown below, starting with the analysis of the classical equation of the solar panel, to then implement the control system along with the perturb & observe algorithm.

The classical solar panel equation as shown in equation 1 is as follows: i_{pv} is the current supplied by the PV module, i_s is the short circuit current which depends on the irradiance, v_{pv} is the operating voltage of the module, $I_R * e^a$ are parameters of the PV module which depend on multiple technological factors and temperature, as shown in figure (7a).

$$i_{pv} = i_{sc} - I_R * e^{a*v_{pv}} \tag{1}$$

To linearize the system we represent it as shown in figure (7b), where the resistor will have the same current and voltage as the classical PV model as found in equation 2, always working at the maximum power point of the MPPT panels.

$$R_{pv} = \frac{v_{mpp}}{i_{pv} - i_{mpp}} \tag{2}$$

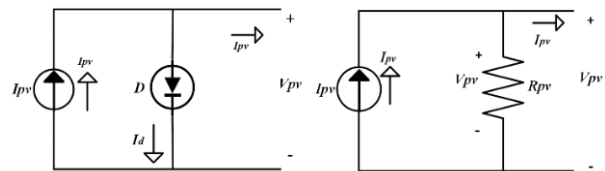


Figure 7a. Figure 7b. Sample of a photovoltaic module with current and voltage variation.
Source: Own elaboration

Based on what has been seen, for the analysis of the system the Norton model is used, already linearised together with the boost converter as shown in figure (8), and thus be able to perform the mathematical modelling around the MPPT maximum power point as proposed by (Hogan, 2014). Circuits comprising arbitrarily complicated sets of voltage sources, current sources, resistors, capacitances and inductances can be represented by Norton equivalent circuits-

According to the above, we see the importance of having a good MPPT algorithm interacting with the various systems involved in a PV, but for the mathematical analysis we must linearise the behaviour of our photovoltaic panel as shown below, starting with the analysis of the classical equation of the solar panel, to then be able to implement the control system together with the perturb & observe algorithm.

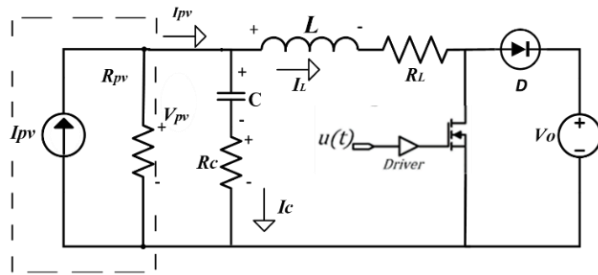


Figure 8 Norton model in a boost converter
Source: Own elaboration

Mathematical analysis

For the mathematical analysis of the system, the objective is to control the input voltage of the PV panel and produce the maximum power, based on the boost converter and considering the losses in both the inductor and the capacitor, adding the series resistors in each of the devices.

For the system analysis, it was performed at two operating points, according to the configuration of the boost converter as shown in figure (8).

To obtain the averaged system, we analysed the boost-boost converter, first in switched mode in its two operations, obtaining the following equations:

$$\begin{cases} u = 1 \text{ in state on} \\ u = 0 \text{ in state off} \end{cases}$$

"u = 1" Interval 1 (switch closed ON)

$$L \frac{dI_L}{dt} = V_C + I_C \times R_C - I_L \times R_L \quad (3)$$

$$C \frac{dV_C}{dt} = I_C = I_{PV} - I_L \quad (4)$$

"u = 0" Interval 2 (switch open OFF)

$$L \frac{dI_L}{dt} = V_C + I_C \times R_C - V_O - I_L \times R_L \quad (5)$$

$$C \frac{dV_C}{dt} = I_C = I_{PV} - I_L \quad (6)$$

Taking into consideration that the generated current I_{PV} and voltage V_{PV} of the Norton model represented in figure (8) are not equations of state as shown in equations (4) and (6) in the analysis of the interval when $u=1$ and $u=0$, these will have to be equated so that the current and voltage of the model are equations of state, by equating these two variables with respect to the Norton model in figure (8) we are left with equations (7) and (8):

$$I_{PV} = I_{SC} - \frac{V_{PV}}{R_{PV}} \quad (7)$$

$$V_{PV} = V_C + I_C \times R_C \quad (8)$$

Substituting equations (7) and (8) into (4) we obtain the following equation which is the same for both system states:

$$C \frac{dV_C}{dt} = \frac{1}{R_{PV} + R_C} (I_{SC} \times R_{PV} - I_L \times R_{PV} - V_C) \quad (9)$$

By performing the relevant operations on equations (3) and (5) for the inductor and (9) for the capacitor in the boost converter, the averaged model looks as follows, where the equations are already a function of the system inputs:

$$L \frac{dI_L}{dt} = V_C + I_C \times R_C - I_L \times R_L - V_O \times (1 - d) \quad (10)$$

$$C \frac{dV_C}{dt} = \frac{1}{R_{PV} + R_C} (I_{SC} \times R_{PV} - I_L \times R_{PV} - V_C) \quad (11)$$

For the steady state analysis, we again consider the Norton model of figure (8) where we study the following points according to the electrical structure of the PV system: taking into account that the average capacitor current is zero, we obtain that the inductor current will be equal to the PV panel current and the maximum power current, the same would be for the panel voltage which will be equal to the capacitor voltage and the maximum power voltage, thus obtaining the following equations (12 and 13).

$$I_L = I_{PV} = I_{MPP} \quad (12)$$

$$V_C = V_{PV} = V_{MPP} \quad (13)$$

From the above we can also derive the duty cycle by equating equation (10) to zero resulting in equation (14).

$$D = 1 - \frac{V_{MPP} - I_{MPP} \times R_L}{V_O} \quad (14)$$

Based on the averaged model, the equations of state and the steady state analysis, we can perform the mathematical modelling using the state space analysis, this analysis is performed for both solar panels, where we define the state vectors x , which are the inductor current I_L and the capacitor voltage V_C , the input vectors u , which are the duty cycle d the output voltage V_O together with the panel current I_{PV} and the control variable y , which is the PV panel voltage V_{PV} as shown in the following equation.

$$x = \begin{bmatrix} I_L \\ V_C \end{bmatrix} u = \begin{bmatrix} d \\ V_O \\ I_{PV} \end{bmatrix} y = [V_{PV}] \quad (15)$$

According to equations (10) and (11) and to the vectors presented in (15), the matrix δ gives us the relationship between the functions and the states, obtaining as a result the following:

$$\delta = \begin{bmatrix} \left(\frac{1}{L}\right) * \left(\frac{-R_{PV} * R_C}{R_{PV} + R_C}\right) - R_L & \left(\frac{1}{L}\right) * \left(1 - \frac{R_C}{R_{PV} + R_C}\right) \\ \left(\frac{1}{C}\right) * \left(\frac{-R_{PV}}{R_{PV} + R_C}\right) & \left(\frac{1}{C}\right) * \left(\frac{-1}{R_{PV} + R_C}\right) \end{bmatrix} \quad (16)$$

Taking equations (10) and (11) with respect to the input vectors $u = \begin{bmatrix} d \\ V_O \\ I_{PV} \end{bmatrix}$ for the matrix β which gives us the relationship between the function and the inputs, we obtain:

$$\beta = \begin{bmatrix} \left(\frac{1}{L}\right) * V_O & \left(\frac{1}{L}\right) * (-1 - d) & \left(\frac{1}{L}\right) * R_C \left(\frac{R_{PV}}{R_{PV} + R_C}\right) \\ 0 & 0 & \left(\frac{1}{C}\right) * \left(\frac{R_{PV}}{R_{PV} + R_C}\right) \end{bmatrix} \quad (17)$$

For the matrix γ , having the variable to control $y = [V_{PV}]$ in terms of the states $x = \begin{bmatrix} I_L \\ V_C \end{bmatrix}$ we obtain:

$$\gamma = \left[R_C \left(\frac{-R_{PV}}{R_{PV} + R_C}\right) \quad 1 - \frac{R_C}{R_{PV} + R_C} \right] \quad (18)$$

For the matrix D , having the variable to be controlled $y = [V_{PV}]$ on the basis of the entries $u = \begin{bmatrix} d \\ V_O \\ I_{PV} \end{bmatrix}$ we obtain:

$$\varepsilon = \left[0 \quad 0 \quad R_C \left(\frac{R_{PV}}{R_{PV} + R_C}\right) \right] \quad (19)$$

As we can see, the state space analysis shows us the complete behaviour of the system to then obtain the transfer functions for both photovoltaic panels, these functions will be explained in the following section.

Comparison between Proportional, Proportional Integral and Proportional Integral Derivative Controls

As we know, to control a variable of a switched converter, it is necessary that the switched converters have a closed loop control system as shown in figure (9), where 4 components can be observed, 1) the main component, which is the switched converter, and 2) the block that calculates the error of the switching converter, 2) the block that calculates the voltage error $e(t)$ which is indispensable for the comparison of the system between what is to be controlled and the error $e(t)$ itself, 3) the control component which mainly acts on the error by amplifying it and 4) the modulator, which transforms the output of the controller into digital signals where they are applied directly to the switches of the switched converter. The modulator block is sometimes considered to be part of the controller block or the plant itself (Méndez, 2018).

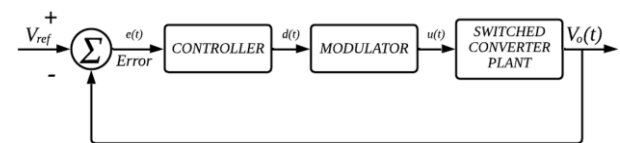


Figure 9 Control block diagram of a switched regulator
Source: Méndez, 2018

Based on the above, for the control design presented in this research we have to consider the following: control the input voltage of the solar panel according to the Norton model, always looking for the maximum MPPT power point together with the control system as shown in figure (10), this will be explained in detail in the following section.

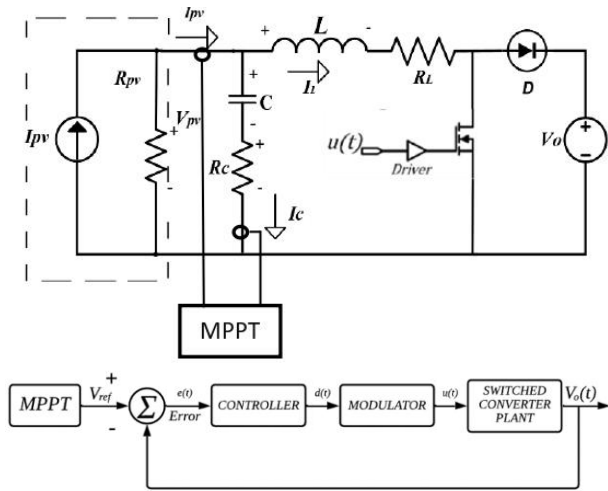


Figure 10 Control block diagram of a switched regulator together with MPPT input
Source: Méndez, 2018

We start with the comparison between the different control systems, explaining why the PI integral proportional control is the one that best suits the needs of the PV system, according to the mathematical analysis explained in the previous section.

Proportional control panel 85W

When proportional control is applied, we can see the following:

Working in closed loop, in figure (11) we can see that it is divided into three parts, the step response, the geometric place of the roots and the Bode diagram: In the Bode diagram we can see that when applying the proportional control the bandwidth never reaches the final value, which is marked by the black line and is the value indicated by the control, in the geometric locus of the roots we can see that the closed-loop poles also do not approach the damping (delimited by the black lines) indicated by the control system even when changing the value of the proportional constant, and although we can see that the response over time reaches a certain stability, at start-up it tends to be oscillatory, so we conclude that proportional control is not a good option for implementation in our system.

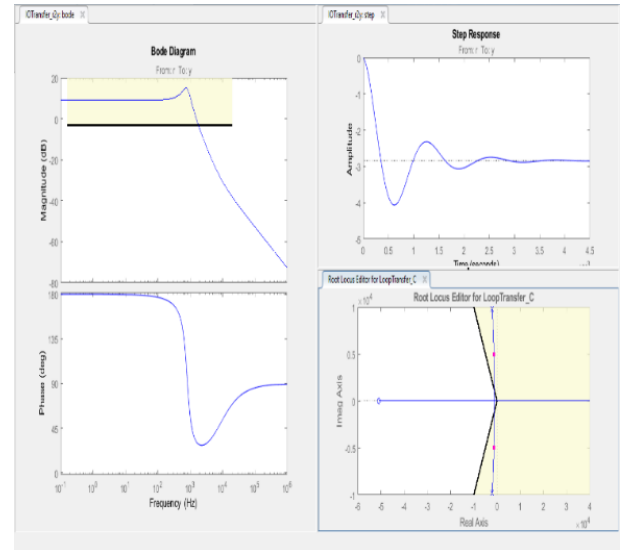


Figure 11 Application of Proportional Control
Source: Own elaboration

Integral proportional derivative control panel 85W

When proportional integral derivative control is applied, we can see the following: in figure (12), we can see in the Bode diagram that the bandwidth does reach the value marked by the control line, but although it complies in this way, graphically we can see that the response is not optimal, in the geometric location of the roots we see that the closed-loop poles are not close to the damping marked by the black lines and that it is difficult to reach it. The response over time, like the proportional control, shows a certain stability, but the response at the start of the system also shows some oscillation.

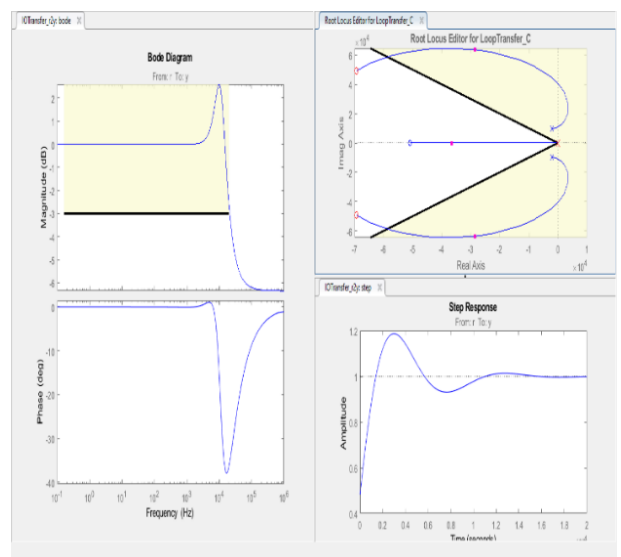


Figure 12 Application of Derivative Proportional Integral Control
Source: Own elaboration

Integral proportional control panel 85W

When the proportional integral control is applied, we can see the following:

According to figure (13), as with the two previous controls, it is shown in the Bode diagram that the bandwidth does reach the value marked by the control line, as does the PID control, but it can be seen that the response is optimal, in the geometric location of the roots we see that the closed-loop poles are now positioned directly on the damping lines marked by the control. The response in time presents a stability and an optimum response for the control system, so we can conclude that the PI control compared to the other controls is the optimum in all the operating conditions that the control system designed.

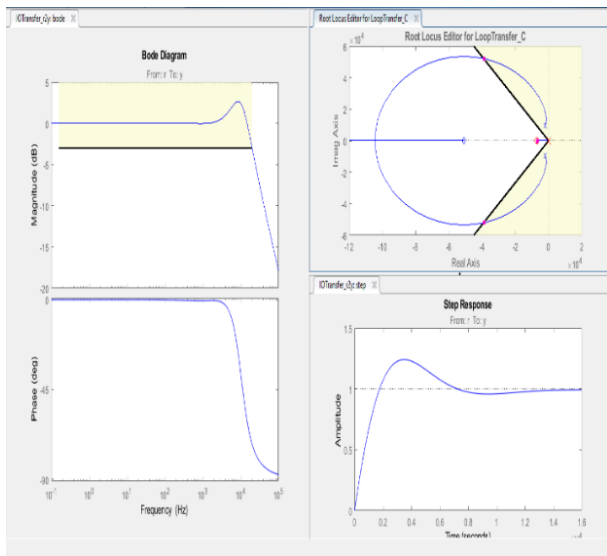


Figure 13 Application of Derivative Proportional Integral Control
Source: Own elaboration

Integral proportional control panel 100W

When proportional control is applied, the following can be seen:

In figure (14) as in the 85W panel working in closed loop: In the Bode diagram we can see that when applying the proportional control the bandwidth never reaches the final value which is marked by the black line and is the value indicated by the control, in the geometrical place of the roots we can observe that the closed loop poles also do not approach the damping (marked by the black lines) indicated by the control system, even changing the value of the proportional constant we do not have a significant approach, and although we see that the response over time reaches a certain stability, at start-up it tends to be oscillatory, so we conclude that the proportional control is not a good option for implementation in our system, very similar to the behavior in the 85W panel.

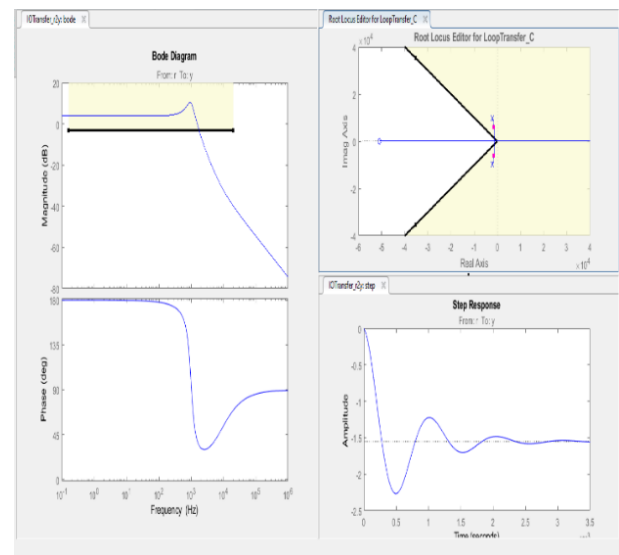


Figure 14 Application of Proportional Control 100 W
Source: Own elaboration

Integral proportional derivative control 100W panel

When proportional integral derivative control is applied, we can see the following:

In the same way we analyze the system presented in figure (15), very similar to the behavior of the 85W panel, so we will summarize it a little, the Bode diagram the bandwidth does reach the value marked by the control line, but although it complies in this way, graphically it can be seen that the response is not the optimum, in the geometrical place of the roots, the closed loop poles are not close to the damping marked by the black lines, and the response in time as well as the proportional control finds some stability but the response at the beginning of the system also presents some oscillation.

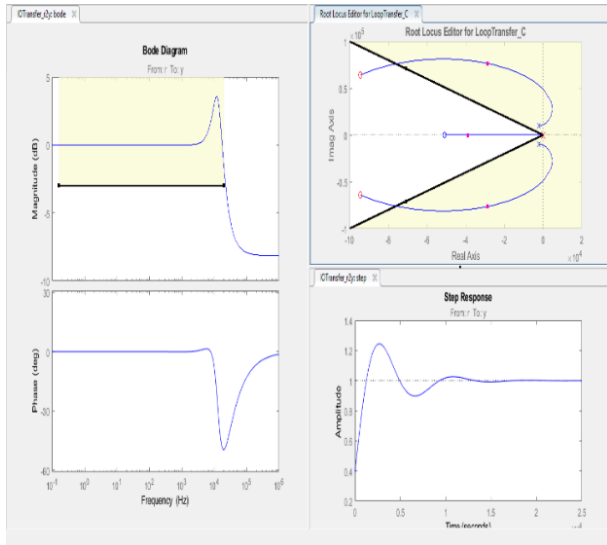


Figure 15 Application of proportional integral derivative control 100 W

Source: Own elaboration

Integral proportional control panel 100W

When the proportional integral control is applied, we can see the following:

According to figure (16), following the same thematic and observing that the behaviour of the control is also very similar to the 85W panel, we can appreciate that in the Bode diagram the bandwidth does reach the value marked by the control line, just like the PID control but it can be observed that the response is optimal. In the geometric location of the roots we see that the closed-loop poles are now positioned directly on the damping lines marked by the control, and the response over time shows stability and an optimum response for the control system, so we can conclude that the proportional integral control is the most optimum for both panels as it meets the operating conditions required by the control system.

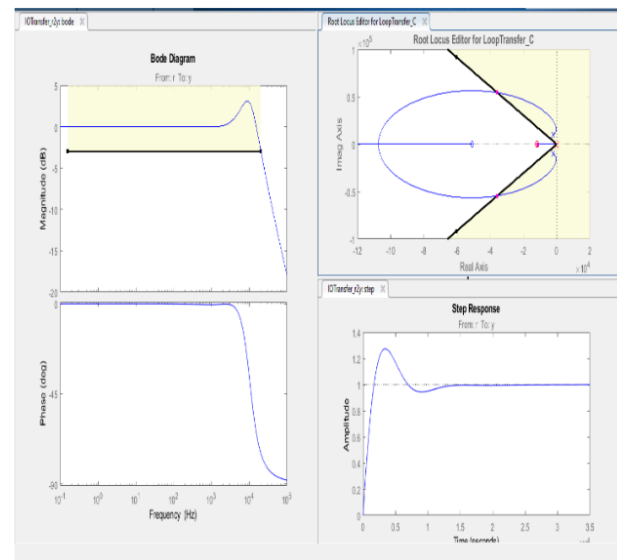


Figure 16 Application of integral proportional control 100 W

Source: Own elaboration

Implementation of control systems

Based on (Méndez, et al., 2015) for the analysis of the first panel we obtain the following technical characteristics; the photovoltaic panel is an 85 W module, with nominal parameters at 25°C and 1 kW / m² of: $I_{SC} = 5$ A, $V_{oc} = 22.1$ V, $I_{MPP} = 4.72$ A, $V_{MPP} = 18$ V. The second panel has the following technical characteristics; it is a 100 W photovoltaic panel with nominal parameters at 25°C and 1 kW / m² of: $I_{SC} = 5.86$ A, $V_{OC} = 22.3$ V, $I_{MPP} = 5.38$ A, $V_{MPP} = 18.6$ V. After the relevant analyses to obtain the parameters of the boost converter, the values for each of the components are as follows: $L=75\mu\text{H}$, $R_L=150\text{m}\Omega$, $C=75\mu\text{F}$, $R_C=196.3\text{m}\Omega$.

Obtaining the transfer functions by performing the analysis prior to modelling the boost converter and linearizing around the operating point in both photovoltaic panels is as follows:

For the 85W panel

$$G_{vd} = \frac{-62641(s+6.791 \cdot 10^4)}{s^2+4817s+1.776 \cdot 10^8} \quad (20)$$

For the 100W panel

$$G_{vd} = \frac{-62515(s+6.791 \cdot 10^4)}{s^2+4947s+1.776 \cdot 10^8} \quad (21)$$

As we can appreciate both transfer functions are very similar, both show that the system is stable, but they present a negative gain, so the system could present some instability, due to this, the control design becomes more complex, as it is left with positive feedback. The control design now must compensate or cancel the negative gain of the system, and with this, have a stable system. By compensating the gain and as shown in the diagrams above from the comparison of the different controls we get the following transfer functions

For the 85W panel

$$G_{cv} = \frac{-1.6317s - 6773}{s} \quad (22)$$

For the 100W panel

$$G_{cv} = \frac{-1.7511s - 1.42 \cdot 10^4}{s} \quad (23)$$

By obtaining the above transfer functions and with the control system applied, we observe that it is completely stable, which allows the objective of the control system to be achieved, which is to regulate the input voltage of the photovoltaic panel following a reference voltage, always looking for the point of maximum power. As shown in the following graphs, we start with the 85W panel and then the 100W panel.

As we can see in figures (17) and (18), the panel operates properly, which proves that the linearisation of the panel is correct, as it is above 18V, which is the optimum operating voltage of the panel according to its technical data sheet, as well as the panel current I_{pv} with a value of 4.72A. We can also observe that it is equal to the inductor current, also fulfilling the IL steady state analysis.

For 85W panel

Steady state analysis:

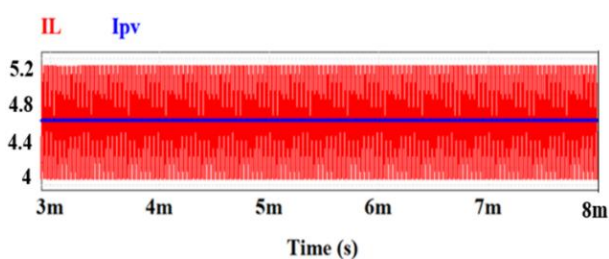


Figure 17 Steady state analysis

Source: Own elaboration

Implemented Control System

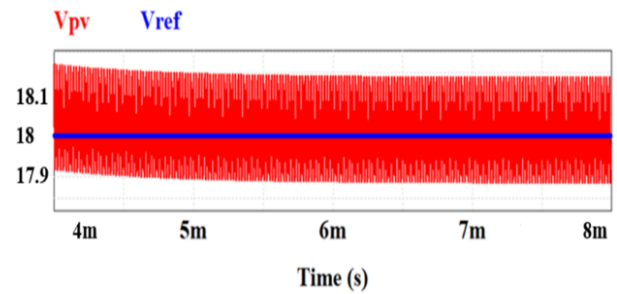


Figure 18 Panel Voltage V_{pv} and Reference Voltage V_{ref}
Source: Own elaboration

In figure (18) we can see that the control operates properly as the panel voltage V_{pv} smoothly follows the reference voltage V_{ref} equal to 18V, always guaranteeing the maximum power point.

Figure (19) shows a direct disturbance to the system simulating a partial shading of the solar panel of almost 70%. The control, when presented with this disturbance, adapts almost immediately and responds again in an optimal way, where it is seen that the voltage V_{pv} of the solar panel after the disturbance continues without problems to the reference voltage V_{ref} always above 18 V, taking into account that the disturbance is quite high the control continues to respond adequately.

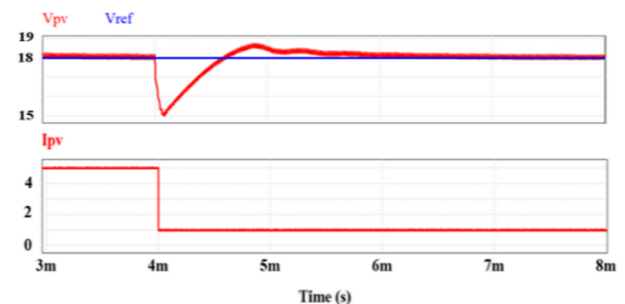


Figure 19 Disturbance present simulating partial shading
Source: Own elaboration

Figure (20) shows another disturbance where there is an increase in the battery voltage due to the load coming from the photovoltaic panel and as can be seen there is an increase in the output voltage V_o from 24V to 27V and again the solar panel voltage V_{pv} follows without any complication the reference voltage V_{ref} always over 18V adapting quickly after the disturbance.

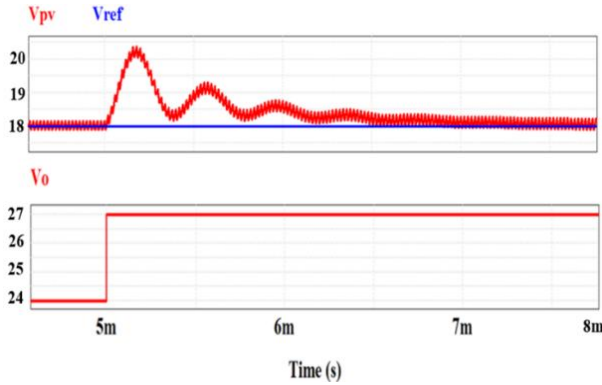


Figure 20 Second disturbance present in the battery
Source: Own elaboration

In the same way as in the 85W solar panel, we can see in figures (21) and (22) now with the 100W solar panel, that it operates properly, which also proves that the linearisation of the panel is correct, as it is above 18.6V and the panel current I_{pv} is equal to the inductor current I_L , also proving the optimal analysis in steady state.

100W panel

Steady state analysis

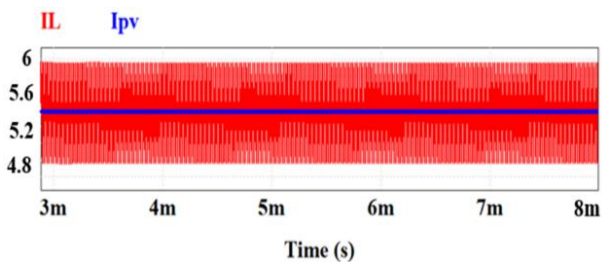


Figure 21 Steady state analysis
Source: Own elaboration

Implemented Control System.

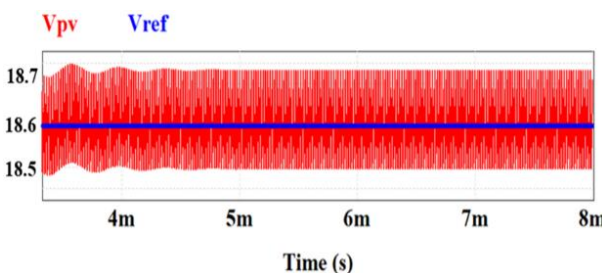


Figure 22 Panel Voltage V_{pv} and Reference Voltage V_{ref}
Source: Own elaboration

As in the previous panel in figure (22) we can see that the control operates properly as the panel voltage V_{pv} smoothly follows the reference voltage V_{ref} now at 18.6V, always ensuring the maximum power point, and the stability of the system.

In figure (23) we repeat the same perturbation that was used in the 85W panel, causing a partial shading of the same magnitude, but now in the 100W panel. As we can observe the I_{pv} current drops its amperage suddenly and considerably, and the control continues to operate correctly, showing the good performance also for this panel.

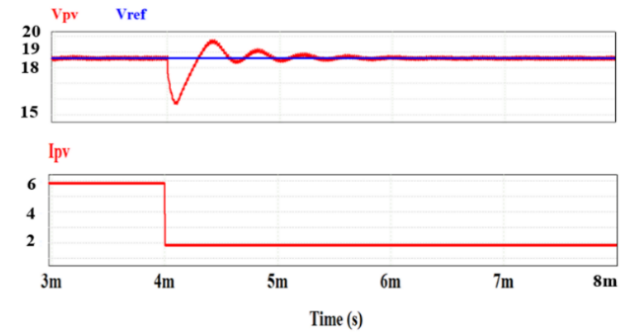


Figure 23 Disturbance present simulating partial shading
Source: Own elaboration

Following the same tests as for the 85W panel, we now show the second disturbance in figure (24) for the 100W panel. The battery load is increased and we observe that the control continues to operate correctly, as the panel voltage V_{pv} continues smoothly at the reference voltage V_{ref} now at 18.6V.

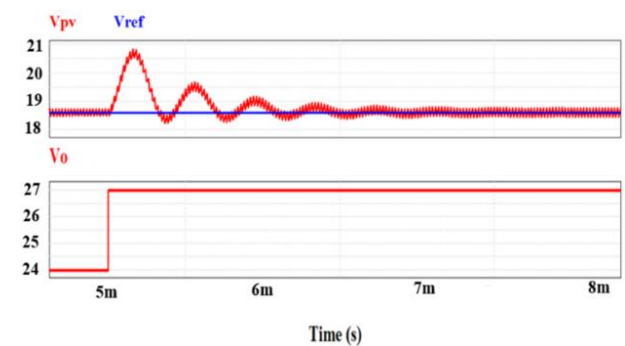


Figure 24 Second disturbance present in the battery

Implementation of the maximum power search algorithm perturb and observe

As we have explained, the techniques for the application of maximum power algorithms are widely used in photovoltaic systems, with the aim of improving the performance of the power output of the photovoltaic system, by constantly monitoring the maximum power point that is directly related to the incidence of radiation and temperature variability in the solar panel. One of the most widely used techniques in photovoltaic systems to obtain maximum power is the perturb and observe algorithm, because it has several advantages, such as low cost and ease of implementation.

In accordance with what has been seen, this article shows the MPPT algorithm based on (Méndez et al., 2015), which is the perturb and observe algorithm, together with the control system already simulated and with the real operation of a solar panel. In the following, the explanation of the perturb-and-observe algorithm is complemented.

The algorithm compares the power obtained for two voltage setpoints separated by a small voltage differential of ± 500 mV. Every 200 μ s the voltage setpoint and power of the first point are replaced by those of the second point, while the voltage setpoint of the second point is obtained by adding the differential to its previous value. The algorithm changes the sign of the differential each time the power of the second point is no longer higher than that of the first point.

Following the same format as the previous figures, we will start by showing the behavior of the 85W panel and then the 100W panel including the implementation of the algorithm.

For the 85W panel

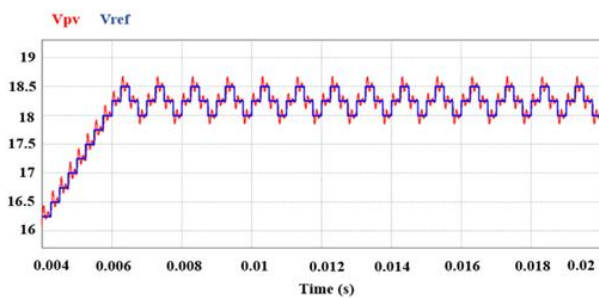


Figure 25 Implementation of the algorithm with the control system Panel Voltage Vpv and Reference Voltage Vref

As we can see in figure (25) by adding the MPPT algorithm to the control system, it works correctly, as the voltage Vpv smoothly follows the reference voltage Vref always looking for the maximum power point of the solar panel.

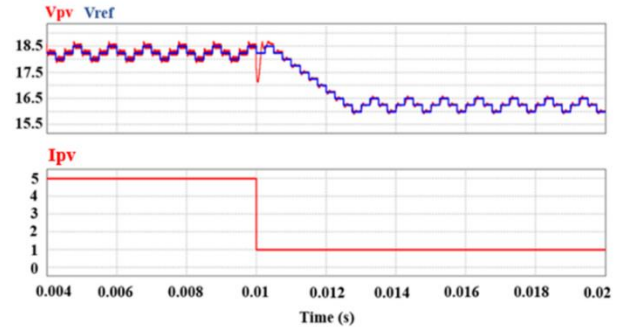


Figure 26 First disturbance present on the solar panel simulating partial shading

Figure (26) shows again a direct disturbance to the system simulating a shading on the solar panel. The control, when presenting this disturbance, adapts almost immediately and responds again in an optimal way, where it can be seen that the voltage Vpv of the solar panel after the disturbance follows without problems the reference voltage Vref, and always looking for the point of maximum power of the MPPT system.

For 100w panel

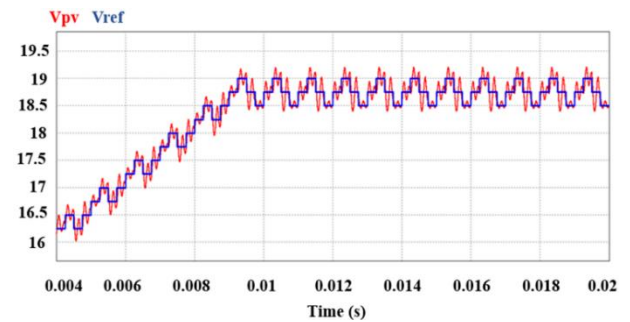


Figure 27 Implementation of the algorithm with the control system Panel voltage Vpv and Reference voltage Vref

As with the 85W solar panel, we can now see on the 100W solar panel that the control together with the application of the MPPT algorithm works correctly.

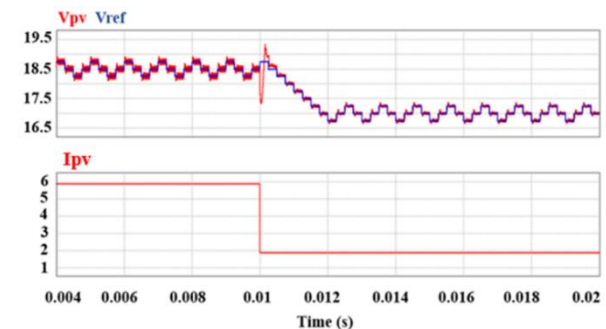


Figure 28 First disturbance present in the solar panel simulating partial shading

The same test that was performed for the 85W solar panel is performed for the 100W panel, provoking a severe disturbance simulating a partial shading and we can observe in figure (28) that the control operates optimally together with the MPPT algorithm, always looking for the maximum power point.

Conclusion

Following the theoretical analysis and verifying with the simulations, we can observe that it is possible to regulate the input voltage of the two photovoltaic panels with the application of a PI controller together with the implementation of the perturb and observe algorithm. Using the MATLAB tool for the design itself, we can deduce that the use of this tool greatly facilitates the design of controllers for application in switched-mode converters, and that it fulfils the objectives set out for this research in an optimal manner. It was also found that by implementing a conventional PI control we can have the same performance of a much more robust control, applied to photovoltaic systems, and that in conjunction with the algorithm proposed in this work, for example, good results are obtained regardless of the existence of disturbances, always operating at the point of maximum power, and as a complement, having other advantages such as easy application, reduced operating time and reduced operating costs when required to implement the model physically.

References

- Ram, J. P., Babu, T. S., & Rajasekar, N. (2017). A comprehensive review on solar PV maximum power point tracking techniques. *Renewable and Sustainable Energy Reviews*, 67, 826–847. <https://doi.org/10.1016/j.rser.2016.09.076>
- Sharma, C., & Jain, A. (2015). Modeling of buck converter models in MPPT using PID and FLC. *Telkomnika (Telecommunication Computing Electronics and Control)*, 13(4), 1270–1280. <https://doi.org/10.12928/TELKOMNIKA.v13i4.1774>
- Ebrahimi, M. J., & Viki, A. H. (2015). Interleaved high step-up DCDC converter with diode-capacitor multiplier cell and ripple-free input current. *International Journal of Renewable Energy Research*, 5(3), 782–788. <https://doi.org/10.11591/eei.v4i4.512>
- Saravanan, S., & Ramesh Babu, N. (2017). Analysis and implementation of high step-up DC-DC converter for PV based grid application. *Applied Energy*, 190, 64–72. <https://doi.org/10.1016/j.apenergy.2016.12.094>
- Alam, K., & Hoque, A. (2019). Design and Analysis of Closed Loop Interleaved Boost Converter with Arduino based Soft PI Controller for Photovoltaic Application. *Proceedings of 2019 3rd IEEE International Conference on Electrical, Computer and Communication Technologies, ICECCT 2019*, 1–5. <https://doi.org/10.1109/ICECCT.2019.8869408>
- Taghvaei, M. H., Radzi, M. A. M., Moosavain, S. M., Hizam, H., & Hamiruce Marhaban, M. (2013). A current and future study on non-isolated DC-DC converters for photovoltaic applications. *Renewable and Sustainable Energy Reviews*, 17, 216–227. <https://doi.org/10.1016/j.rser.2012.09.023>
- Dhople, S. V., Davoudi, A., & Chapman, P. L. (2009). Steady-state characterization of multi-phase, interleaved Dc-Dc converters for photovoltaic applications. *2009 IEEE Energy Conversion Congress and Exposition, ECCE 2009*, 330–336. <https://doi.org/10.1109/ECCE.2009.5316415>
- Tian, X., Zheng, M., & Yang, S. (2016). Maximum power point tracking for photovoltaic power based on the improved interleaved boost converter. *Proceedings of the 2016 IEEE 11th Conference on Industrial Electronics and Applications, ICIEA 2016*, 1, 2215–2218. <https://doi.org/10.1109/ICIEA.2016.7603957>
- Dwivedi, L. K., & Saket, R. K. (2017). Improve efficiency of Photovoltaic (PV) system based by PID controller. *International Research Journal of Engineering and Technology*, 4(5), 2273–2277. <https://www.irjet.net/volume4-issue05>
- Rabiaa, O., Mouna, B. H., Lassaad, S., Aymen, F., & Aicha, A. (2019). Cascade Control Loop of DC-DC Boost Converter Using PI Controller. *International Symposium on Advanced Electrical and Communication Technologies, ISAECT 2018 - Proceedings, May 2019*, 1–5. <https://doi.org/10.1109/ISAECT.2018.8618859>

Mendez-Diaz, F.; Ramirez-Murillo, H.; Garces, P.; Romero, A.; Calvente, J.; Giral, R. (2014). Control en Modo de Deslizamiento de la Tensión de Entrada del Convertidor Buck - Boost. June, 1–6

<http://deeea.urv.cat/gaei/publications.html#2014>

Mendez-Diaz, F., Ramirez-Murillo, H., Calvente, J., Pico, B., & Giral, R. (2015). Input voltage sliding mode control of the versatile buck-boost converter for photovoltaic applications. Proceedings of the IEEE International Conference on Industrial Technology, 2015-June(June), 1053–1058. <https://doi.org/10.1109/ICIT.2015.7125236>

Méndez Díaz, J. F. (2018). Desarrollo de un Sistema de Iluminación Solar Para el Ahorro de Energía Eléctrica en el Alumbrado Público de México. UNIVERSITAT ROVIRA I VIRGILI, UNIVERSIDAD POPULAR AUTONOMA DEL ESTADO DE PUEBLA <http://hdl.handle.net/10803/667293>

Mendez-Diaz, F., Pico, B., Vidal-Idiarte, E., Calvente, J., & Giral, R. (2019). HM/PWM Seamless Control of a Bidirectional Buck-Boost Converter for a Photovoltaic Application. IEEE Transactions on Power Electronics, 34(3), 2887–2899. <https://doi.org/10.1109/TPEL.2018.2843393>

Bouchakour, A., Zaghba, L., Brahami, M., & Borni, A. (2015). Study of a Photovoltaic System Using MPPT Buck-Boost Converter. International Journal of Materials, Mechanics and Manufacturing, 3(1), 65–68. <https://doi.org/10.7763/ijmmm.2015.v3.168>

Leuchter, J., Zaplatilek, K., & Bauer, P. (2012). Photovoltaic model for circuit simulation. IECON Proceedings (Industrial Electronics Conference), 5399–5405. <https://doi.org/10.1109/IECON.2012.6389526>

Hogan, N. (2014). A general actuator model based on nonlinear equivalent networks. IEEE/ASME Transactions on Mechatronics, 19(6), 1929–1939. <https://doi.org/10.1109/TMECH.2013.2294096>

Ayop, R., & Tan, C. W. (2018). Design of boost converter based on maximum power point resistance for photovoltaic applications. Solar Energy, 160(November 2017), 322–335. <https://doi.org/10.1016/j.solener.2017.12.016>

Shanthi, N., Nivethitha, P., Sindhuja, S., Hilarini, M., & Divyabharathi, K. (2018). High Efficient Interleaved Boost Converter for Photovoltaic Applications. 7th IEEE International Conference on Computation of Power, Energy, Information and Communication, ICCPEIC 2018, 305–308. <https://doi.org/10.1109/ICCPEIC.2018.8525145>

Sizing of the photovoltaic system for a house located in the Presa la Concepción subdivision in Santiago Cuautlalpan, State of Mexico

Dimensionamiento del sistema fotovoltaico para una vivienda ubicada en el fraccionamiento Presa la Concepción en Santiago Cuautlalpan, Estado de México

HERNÁNDEZ-GÓMEZ, Víctor Hugo†*, MORILLÓN-GÁLVEZ, David, OLVERA-GARCÍA, Omar and GUZMAN-TINAJERO, Pedro

Universidad Nacional Autónoma de México, FES Cuautitlán, Estado de México, México.

ID 1st Author: *Víctor Hugo, Hernández-Gómez* / ORC ID: 0000-0001-9315-5869, Researcher ID Thomson: S-6575-2018, CVU CONAHCYT ID: 122247

ID 1st Co-author: *David, Morillón-Gálvez* / ORC ID 0000-0002-9178-3092, Researcher ID Thomson S-6702-2018, CVU CONAHCYT ID: 253013

ID 2nd Co-author: *Omar, Olvera-García* / ORC ID: 0000-0001-6386-9772, Researcher ID Thomson: S-6644-2018, CVU CONAHCYT ID: 706478

ID 3rd Co-author: *Pedro, Guzman-Tinajero* / ORC ID: 0000-0002-2297-7758, arXiv Author ID: PEDRO_GUZMAN_T, CVU CONAHCYT ID: 251228

DOI: 10.35429/JEE.2023.18.7.27.30

Received January 20, 2023; Accepted June 30, 2023

Abstract

To cover the needs of the human being, either electrical or thermal energy is used, which causes greenhouse gases due to the origin of the energy, since most of it is generated by burning fossil fuels. It is necessary to change the source of energy for others that are not polluting, that is, for renewable energies. In a house, energy consumption is in electrical appliances, lighting, air conditioning, entertainment equipment, stove and boiler. In a previous study, strategies were proposed for the passive air conditioning of a house in the Fraccionamiento de Presa la Concepción located in Santiago Cuautlalpan, State of Mexico, considering the bioclimate of the place. In the present study, the photovoltaic system required to cover the energy demand of that house is proposed. The characteristics of the home are briefly described (location, installed load and the bi-monthly consumption reported by CFE), the methodology to be followed for the sizing of the system and its application. A proposal of solar panels, inverter and battery to be used with their respective costs is given.

Resumen

Para cubrir las necesidades del ser humano, se utiliza energía ya sea eléctrica o térmica, lo que ocasiona gases de efecto invernadero por el origen de la energía, ya que la mayor parte de ella se genera por quema de combustibles fósiles. Es necesario cambiar la fuente de energía por otras que no sean contaminantes, es decir, por las energías renovables. En una casa habitación, el consumo de energía está en los electrodomésticos, iluminación, aire acondicionado, equipos para diversión, estufa y boiler. En un estudio anterior, se propusieron estrategias para la climatización pasiva de una vivienda del Fraccionamiento de Presa la Concepción ubicado en Santiago Cuautlalpan, Estado de México, considerando el bioclima del lugar. En el presente estudio, se propone el sistema fotovoltaico requerido para cubrir la demanda energética de esa vivienda. Se describe brevemente las características de la vivienda (ubicación, carga instalada y el consumo bimestral reportado por CFE), la metodología a seguir para el dimensionamiento del sistema y su aplicación. Se da una propuesta de paneles solares, inversor y batería a emplear con sus respectivos costos.

Photovoltaic, Energy saving, passive systems

Fotovoltaico, Ahorro de energía, Sistemas pasivos

Citation: HERNÁNDEZ-GÓMEZ, Víctor Hugo, MORILLÓN-GÁLVEZ, David, OLVERA-GARCÍA, Omar and GUZMAN-TINAJERO, Pedro. Sizing of the photovoltaic system for a house located in the Presa la Concepción subdivision in Santiago Cuautlalpan, State of Mexico. Journal Electrical Engineering. 2023. 7-18:27-30.

* Author's Correspondence (E-mail: vichugo@unam.mx)

† Researcher contributing as first author.

Introduction

The energy consumed in a house is usually thermal energy (used for food preparation or for heating water for bathing) or electrical energy (for household appliances and electronic devices), which are generated through fossil fuels, which, when burned, generate greenhouse gases that cause serious environmental pollution problems, such as global warming, climate change, changes in ocean currents, rising sea levels, etc. It is necessary to look for alternatives that allow us to cover our energy needs without causing problems to the environment.

The use of air conditioning systems are examples of energy consumption in homes, where not only the initial investment of the equipment is paid, but also the bimonthly consumption of the electricity bill. Hernández et al (2022) proposed strategies for the passive air conditioning of a house in the Presa la Concepción housing development located in Santiago Cuautlalpan, State of Mexico. With the data of the location of the house, the bioclimate of the place and the characteristics of the building envelope, they determined the temperature and hourly humidity tables of the place and established the thermal comfort zone. They determined the psychrometric process involved, the resulting heat balance due to sensible heat gains by occupants, equipment, solar radiation and environment, and finally, the air flow required by the equipment. They proposed strategies, considering thermal insulation, coatings and passive systems.

The present study, takes up the house located in the Presa la Concepción subdivision, to dimension a photovoltaic system that is capable of covering its electrical energy demand.

Location and climate

The Hacienda la Concepción subdivision is located in the vicinity of the La Concepción dam, in Santiago Cuautlalpan, State of Mexico, with a latitude of 19.685° , longitude of -99.286° and altitude of 2,340 m above sea level.

Solar radiation data were obtained from the weatherspark.com page, where statistical analysis of historical hourly climatological reports and model reconstructions from January 1, 1980 to December 31, 2016 of the four stations near Santiago Cuautlalpan is performed.

The statistical data mention that from March 9 to June 6 has the season with the highest solar radiation presenting average values greater than 6.9 kWh/m^2 , being April the month that receives the highest radiation with average values of 7.3 kWh/m^2 . From November 8 to January 25 is the period with the lowest direct radiation with average values of less than 5.4 kWh/m^2 , with December having the lowest average value of 5.0 kWh/m^2 . Table 1 shows the average values of solar radiation and cloud cover.

	Jan	Feb	Mar	Apr	may	jun	jul	aug	sep	oct	nov	dec
Solar energy kWh	53	62	70	74	72	65	63	62	58	57	53	50
Cloudy %	40	34	35	40	49	75	84	85	87	72	49	44
Clear %	60	66	65	60	51	25	16	15	13	28	51	56

Table 1 Monthly average incident radiation and cloudiness of Santiago Cuautlalpan

Source: <https://es.weatherspark.com/y/5666/Clima-promedio-en-Santiago-Cuautlalpan-M%C3%A9xico-durante-todo-el-a%C3%B1o>

Characteristics of the house

The property shown in Figure 1 has two levels and has a total area of 317.836 m^2 .



Figure 1 Facade of the house

Source: Own elaboration

Table 2 shows a list of the equipment that consumes electrical energy at the site, giving a total of 3005 W of total installed load.

First floor	Power W	Quantity	Subtotal W
40 inch TV	90	1	90
Blu-ray	34	1	34
Stove	635	1	635
Refrigerator	400	1	400
Washing machine	800	1	800
Light bulbs	25	12	300
		Total	2259
First level	Power W	Quantity	Subtotal W
40-inch TV	90	4	360
Blu-ray	34	4	136
Spotlights	25	10	250
Lap top		3	0
		Total	746
		Total	3005

Table 2 Equipment installed in the house
Source: Own elaboration

In order to know the annual consumption (KWh) of the house, the electricity bills provided by CFE on a bimonthly basis were considered. Table 3 shows the data provided by the electricity bills for the years 2021, 2022 and 2023 of the house.

Period	KWH	\$	KWH ANUAL
03 FEB 23 to 04 APR 23	326	\$ 569.00	
06 DEC 22 to 03 FEB 23	295	\$ 431.00	
05 OCT 22 to 06 DEC 22	368	\$ 732.00	
03 AUG 22 to 05 OCT 22	399	\$ 851.00	
03 JUN 22 to 03 AUG 22	354	\$ 657.00	
05 APR 22 to 03 JUN 22	340	\$ 593.00	2198
02 FEB 22 to 05 APR 22	358	\$ 658.00	
02 DEC 21 to 02 FEB 22	379	\$ 734.00	
06 OCT 21 to 02 DEC 21	347	\$ 601.00	
02 AUG 21 to 06 OCT 21	435	\$ 822.00	
02 JUN 21 to 02 AUG 21	361	\$ 598.00	2449
05 APR 21 to 02 JUN 21	377	\$ 708.00	
02 FEB 21 to 05 APR 21	438	\$ 938.00	
01 DEC 20 to 02 FEB 21	491	\$1,136.00	
AVERAGE	376	\$ 716.29	2323.5

Table 3 Bimonthly consumption taken from CFE bills
Source: Own elaboration

Since the pandemic forced people to stay in their homes, this increased electricity consumption for the year 2021, in order to have an estimate without pandemic, for the study we will consider the consumption of the year 2022, which was 2198 kWh, equivalent to 6022 Wh per day.

Methodology

For the sizing of the photovoltaic system, we will perform the following:

Determination of the number of photovoltaic panels

Determination of the number of batteries to be used

Angle of inclination of the panels.

Dimensioning of the photovoltaic system.

To determine the number of photovoltaic panels we will use equation 1:

$$Np = \frac{\text{Average daily consumption Wh} \times \text{Safety factor}}{\text{Panel power in W} \times \text{Peak sun hours h}} \quad [1]$$

The average daily consumption is 6022 Wh, for the safety factor, in the literature it is recommended to use values between 1.25 to 1.3, so for the study we will use 1.3.

For the power of the photovoltaic panel, there is already a great variety of photovoltaic panels on the market, which can be monocrystalline or polycrystalline. From a search, the Greenlux brand monocrystalline panel with a power of 540 W and a current of 9.67 A was selected.

The hours of peak sunshine are the number of hours in which we have a hypothetical constant solar irradiance of 1000 W/m² on the photovoltaic panel. According to data from the Geographic Information System for Renewable Energies in Mexico (SIGER IIE-GENC) and the Solar Radiation Observatory of the Institute of Geophysics of the UNAM, the peak sunshine hours for a surface inclined to the latitude of the State of Mexico is 6.09 h. Therefore,

$$Np = \frac{6022 \text{ Wh} \times 1.3}{540 \text{ W} \times 6.09 \text{ h}} = 2.38$$

That is, 3 photovoltaic panels of 540 W of power are required.

When designing a photovoltaic system, it is necessary to consider backup batteries for the use of energy when there is no solar radiation, for example at night. To determine the capacity of the batteries, equation 2 is considered:

$$Cb = \frac{\text{Average daily consumption} \times \text{Days of autonomy D}}{\text{Depth of discharge} \times \text{Battery voltage V}} \quad [2]$$

The autonomy of the system considers the time we want to use the capacity of the battery when there is no light supply, for the study was considered half a day.

Also, from a search in the market, the battery that was selected for the system was the NM gel 12V - 230Ah, with a depth of discharge of 0.6. Therefore, the battery capacity will be:

$$C_b = \frac{6022 \text{ Wh} \times 0.5 D}{0.6 \times 12 \text{ V}} = 418.9 \text{ Ah}$$

The number of NM gel batteries to occupy is calculated with equation 3:

$$N_B = \frac{\text{Required capacity Ah}}{\text{Battery capacity Ah}} = \frac{418.9 \text{ Ah}}{230 \text{ Ah}} = 1.82 \quad [3]$$

That is, 2 batteries of 230 Ah are required to cover the demand for half a day.

For the installation of the system, the tilt angle of the PV panel is calculated with equation 4:

$$\text{Inclination} = 3.7 + (0.69 \times \text{latitude}) \quad [4]$$

Therefore:

$$\text{Inclination} = 3.7 + (0.69 \times 19.685) = 17.28^\circ$$

For the location of the house with 19.685° latitude, the inclination of the photovoltaic panel should be 17.28° .

The Huawei top 5 world top 5 inverter 6.0KWP was selected for the system.

Table 4 shows the approximate costs of the selected equipment.

	Cost	Quantity	Subtotal
Solar panel	\$ 12,000.00	3	\$ 36,000.00
Battery	\$ 9,000.00	2	\$ 18,000.00
Inverter	\$ 40,200.00	1	\$ 40,200.00
		Total	\$ 94,200.00

Table 4. System costs

Source: Own.

Conclusions

The use of renewable energies to reduce the consumption of fossil fuels is a good alternative, although the investment cost could be high, in the long run this cost can be reduced with what is no longer paid every two months for the cost of energy, in addition, with the support of the CFE modality of Home Interconnection Contract, the energy generated during the day and not used can be sold, for example, when everyone goes out to do their daily activities, increasing the recovery of the investment.

Acknowledgement

Work carried out with the support of the Internal Program of Research Chairs (FES Cuautitlán - UNAM), for the support provided through project CI2252.

Work carried out with the support of the UNAM-DGAPA-PAPIME PE100222 Program.

References

HERNÁNDEZ-GÓMEZ, Víctor Hugo, MORILLÓN-GÁLVEZ, David, OLVERA-GARCÍA, Omar and GUZMAN-TINAJERO, Pedro. Strategies for passive air conditioning and energy saving of a house considering the bioclimate of the place. *Journal Architecture and Design*. 2022. 6-15:1-12. DOI: 10.35429/JAD.2022.15.6.1.12.

Design of a bidirectional converter for charging/discharging a supercapacitor**Diseño de un convertidor bidireccional para la carga/descarga de un supercapacitor**

GARZA-GONZÁLEZ, Williams†*, DURÁN-GÓMEZ, José Luis, LÓPEZ-FLORES, David Ricardo and SÁENZ-VALVERDE, David Alberto

Tecnológico Nacional de México campus Chihuahua, México.

ID 1st Author: Williams, Garza-González / **ORC ID:** 0000-0001-9668-7780, **CVU CONACYT ID:** 1079314

ID 1st Co-author: José Luis, Durán-Gómez / **ORC ID:** 0000-0003-0904-7828, **CVU CONAHCYT ID:** 11985

ID 2nd Co-author: David Ricardo, López-Flores / **ORC ID:** 0000-0003-4016-0845, **CVU CONAHCYT ID:** 250204

ID 3rd Co-author: David Alberto, Sáenz-Valverde / **ORC ID:** 0009-0007-7729-4077, **CVU CONAHCYT ID:** 1202447

DOI: 10.35429/JEE.2023.18.7.31.39

Received January 25, 2023; Accepted June 30, 2023

Abstract

This article presents the analysis and design of a new converter that combines the current doubler topology and the parallel converter to achieve greater stability and effective reduction of ripple in both voltage and current parameters. Basically, the DC-DC (Direct Current to Direct Current) converter operates with pulse modulators to control the current in the desired charging or discharging direction. Extensive simulations were carried out at nominal values of 48 V and 8.5 A of output, and 100 V of input to confirm the performance of this converter. The approach used has benefits in terms of safety, reduced electrical noise, practical implementation for interconnecting energy sources with high voltage ratios, and increased lifespan of supercapacitors as well as batteries. Simulation results are presented and the advantages and applications of this new configuration are discussed.

Resumen

Este artículo presenta el análisis y diseño de un nuevo convertidor que combina la topología del doblador de corriente y el convertidor paralelo para lograr una mayor estabilidad y una reducción efectiva del rizo en ambos parámetros de tensión y corriente. Básicamente el convertidor de CD-CD (Corriente directa a corriente directa) operara con moduladores de pulso para dirigir la corriente en el sentido deseado de carga o descarga. Se realizaron extensas simulaciones en valores nominales de 48 V y 8.5 A de salida, y 100 V de entrada para confirmar el rendimiento de este convertidor. El enfoque utilizado tiene beneficios en términos de seguridad, menor ruido eléctrico, una implementación práctica para interconectar fuentes de energía con altas relaciones de tensión y un aumento en la vida útil de los supercapacitores, así como de baterías. Se presentan los resultados de simulación y se discuten las ventajas y aplicaciones de esta nueva configuración.

Supercapacitor, Bidirectional, Energy**Supercapacitor, Bidireccional, Energía**

Citation: GARZA-GONZÁLEZ, Williams, DURÁN-GÓMEZ, José Luis, LÓPEZ-FLORES, David Ricardo and SÁENZ-VALVERDE, David Alberto. Design of a bidirectional converter for charging/discharging a supercapacitor. Journal Electrical Engineering. 2023. 7-18:31-39.

* Correspondence to Author (E-mail: M20061554@chihuahua.tecnm.mx)

† Researcher contributing as first author.

Introduction

Today, new technological developments and population growth have led to a significant increase in global electricity consumption. As a result, fossil fuel-based sources of electricity such as gas, oil and coal have increased to meet the world's electricity consumption. Consequently, the environment has been adversely affected due to the increase in greenhouse gases. One alternative to reduce this effect is renewable energy sources (RESs) such as solar or wind power. However, due to the fluctuating and intermittent nature of RESs, it is necessary to equip them with energy storage systems (ESS) to improve their overall efficiency, reliability, and power quality (Hidalgo-Reyes et al., 2019).

For this reason, energy storage devices are becoming very essential elements to take advantage of these renewable energy sources; because their purpose is to store energy for use in times when energy is not produced and thus increase the efficiency of the system. Among all these devices are supercapacitors, which are a technology that is capable of delivering high power pulses in an instant of time; in addition to supporting a large number of charge and discharge cycles as well as providing high efficiency during this process, but despite this they have the disadvantage of being unable to maintain the same voltage for a long time. (Hidalgo-Reyes et al., 2019), due to the above described, power converters are required to regulate to a certain desired voltage.

Direct current to direct current (dc-dc) converters are now being widely used in such applications, since they can be used both to store energy and to help the system deliver energy when it is not generating it, thus offering greater autonomy to power grids, as well as superior sustainability to renewable energy sources.

In recent years, different configurations of bidirectional DC-DC converters have been proposed for supercapacitors. In (Rico-Secades et al., 2016) elaborated a one-branch bidirectional converter (switch array) for charging and discharging two battery modules, using complementary pulse modulator (PWM) circuits in the transistors used; thus allowing that with a small duty cycle the battery is discharged and a larger duty cycle will cause its respective charge.

At (Huang et al., 2018; Ibanez et al., 2013; Kim & Sul, 2006) they propose a 3-branch and 4-branch step-up parallel converter, each branch uses the same duty cycle, but has an offset of 120 and 90 degrees respectively between each of them, this with the purpose of reducing the ripple of the current in the supercapacitors and even if one of the branches presents a failure, the system will be able to remain operational. In (López-Flores et al., 2010) present a phase-shifting full-bridge converter, in which they use the current doubler to be able to deliver a greater amount of current while helping to reduce the ripple, although it depends on the duty cycle used. There are also (Kayaalp et al., 2016; Lai et al., 2016; Shreelekha & Arulmozhi, 2016; Zhixiang Ling et al., 2015) which use phase-shift control, rather than duty-cycle control, thus enabling their more efficient use in multiport systems; (Rahimpour & Baghrmian, 2017; Zakis et al., 2012) use the Z-source and Γ -source topologies for greater voltage and current stability, while reducing the reactive components of the circuit.

The previously analyzed works present appropriate activation methods for the switches of bidirectional dc-dc converters, and thus properly achieve the stability of the operating voltage and current at terminals with an acceptable ripple in both parameters. However, the ripple in the operating voltage and current can be variable and higher.

This paper presents a converter in which the current doubler topology is used in conjunction with the parallel converter topology (Figure 1), where the latter will operate at a duty cycle close to 0.5. Moreover, complementary PWMs circuits are used for a simple and efficient control of the charging and discharging of a supercapacitor (Not addressed in this paper). This approach leads to the following contributions:

- i. Stability in the operating voltage and current of the bidirectional dc-dc converter, as well as effective ripple reduction in both parameters. This results in a positive impact on the lifetime of ESS systems (e.g. batteries and SCs).

- ii. Easy and practical implementation of the bidirectional dc-dc converter for interconnecting two power sources with high voltage ratios (e.g. ESS systems and RESs).

The implicit benefits of the approach used in the proposed bidirectional dc-dc converter are: personnel safety, reduced electrical noise.

In this article the following sections are presented; in section II a detailed analysis of the converter to be studied is made, as well as the obtaining of the different values of each component of the circuit; in section III the simulation results of such proposed circuit are presented, as well as the power semiconductor devices MOSFETs that were selected; in section IV the respective conclusions of the results obtained are exposed; and in section V the literature used is shown.

DC-DC Converter Analysis and Design

In order to implement the converter, a steady-state analysis of the converters will be performed separately and in a forward direction (supercapacitor as a load), taking into account that the transistors T_3 and T_4 (see Figure 1) will have duty cycles complementary to T_2 and T_1 respectively, and S_3 y S_4 with respect to S_1 and S_2 ; the simulation results are presented in the following sections.

I. Two-Branch Parallel Converter

The two-branch parallel converter as explained above will be used only to decrease the current ripple to near zero percent and as this depends on the direction in which it will be used, then it can operate as a boost or buck converter.

Although in the buck mode and with the phases shifted 180 degrees between the two branches, then the output current ripple can be reduced as far as the duty cycle is increased. The maximum point where the current ripple is almost zero is when the sum of each duty cycle of each branch gives one, i.e., 0.5.

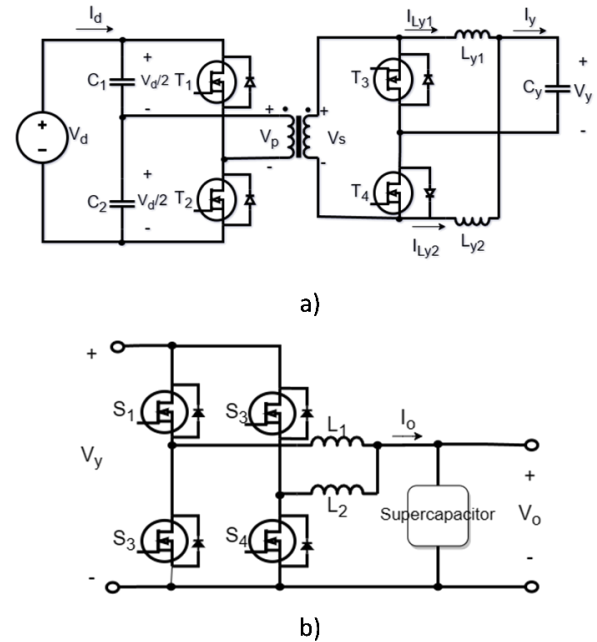


Figure 1 Schematic diagram of proposed topologies a) half-bridge converter complete with current doubler, b) two-branch parallel converter

Source: Own elaboration

For the design of the proposed converter, its voltage gain will be determined first, taking into account that the phase shift must be 180 degrees and the inductors of the same value, so analyzing one of the branches is more than enough.

When the switch S_1 is on the current flows through it and the transistor S_3 will be off, therefore, the inductor current I_{L1} is increased. This increase corresponds to a positive slope current ripple at L_1 , which can be determined by the following equation:

$$\Delta i_{L1(ON)} = \frac{1}{L_1} (V_y - V_o) D_2 T_s \quad (1)$$

where D_2 represents the duty cycle, T_s the switching period, V_o the output voltage at the supercapacitor and V_y the input voltage. Now when the switch S_1 is turned off, then the current through the inductor L_1 , is decremented by means of switch, S_3 , resulting in a curl with negative slope, and (2) represents it in mathematical form.

$$\Delta i_{L1(OFF)} = \frac{1}{L_1} (-V_o) (1 - D_2) T_s \quad (2)$$

Since both the increase and decrease in current ripple is of the same magnitude, therefore, the voltage gain can be determined by equating the absolute values of (1) and (2) as defined in (3).

$$\frac{V_o}{V_y} = D_2 \quad (3)$$

II. Half-Bridge Converter with Current Doubler

The design consists of four transistors (T_1 , T_2 , T_3 and T_4), two input capacitors (C_1 and C_2), one output capacitor (C_y) and two output inductors (L_{y1} and L_{y2}) and a transformer with two windings, as depicted in Figure 1B. The duty cycle of the transistors T_1 and T_2 in which it can operate is from 0 to 0.5, above that value a short circuit is caused between them. Since the inductors are connected to the ends of the secondary winding, then their currents will be 180 degrees out of phase, causing the ripple to decrease as the duty cycle increases.

As long as it is held on T_2 a voltage of $\frac{V_d}{2}$ will be present in the primary, consequently the secondary will have a voltage defined at (4) and the transistor T_3 will remain off, causing in the inductor L_{y1} an increase of the current $I_{L_{y1}}$ according to (5).

$$v_s = \frac{N_2 V_d}{N_1 2} \quad (4)$$

$$\Delta i_{L_{y1}(ON)} = \frac{1}{L_{y1}} \left(\frac{N_2 V_d}{N_1 2} - V_y \right) D_1 T_s \quad (5)$$

Taking into account the above considerations, it can be calculated the variation of the current at L_{y1} as long as T_3 remains in on state (6),

$$\Delta i_{L_{y1}(OFF)} = \frac{1}{L_{y1}} (-V_y)(1-D_1)T_s \quad (6)$$

Performing in a similar way to how it is obtained (3) it is possible to obtain the voltage dc gain from (7).

$$\frac{V_y}{V_d} = \frac{N_2 D_1}{N_1 2} \quad (7)$$

As the two converters (Figures 1a and 1b) are cascaded connected, therefore, the gains are multiplied, thus obtaining the gain between the output and input voltage as,

$$\frac{V_o}{V_d} = \frac{I_d}{I_o} = \frac{1 N_2}{2 N_1} D_1 D_2 \quad (8)$$

Regarding the value of the capacitor, the voltage V_y ripple must be calculated and for this it must first calculate the ripple of the current I_y , since in the sum of the current of the inductors the ripple decreases, then according to the Figure 2 the output current ripple is determined from (9).

$$\Delta I_y = \frac{V_y}{L_{y1} f_s} (1-2D_1) \quad (9)$$

Therefore, the ripple of the capacitor is defined as follows (10).

$$\frac{\Delta V_y}{V_y} = \frac{(1-2D_1)}{16L_{y1} C_y f_s^2} \quad (10)$$

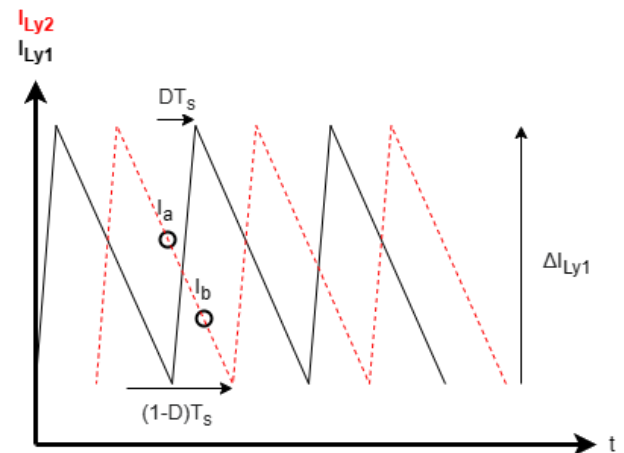


Figure 2 Variation of the currents with respect to time in inductors L_{y1} y L_{y2}

Source: Own elaboration

III. Relationship of Inductor Currents to Output Current

It is easy to deduce from Figure 1 (b) that I_o is the sum of the currents of the inductors L_{y1} y L_{y2} and as both currents have the same waveform, except that they are 180 degrees out of phase; therefore, the average value of the output current is equal to the sum of the two currents of these inductors which leads to significantly reduce the output ripple of I_o of the two-branch parallel converter.

To obtain a mathematical expression that relates I_o to the current of L_{y1} , it is first necessary to know the waveform of current that pass over S_3 , which according to Figure 3 the average current flowing through S_3 can be defined as,

$$I_{S3} = \left[\frac{1}{2} \Delta I_{L1} (1-D_2) T_s \right] \frac{1}{T_s} + \left[\widetilde{I}_{L1} (1-D_2) T_s \right] \frac{1}{T_s} \quad (11)$$

Simplifying (11) it is obtained the current in I_{S3} as shown,

$$I_{S3} = I_{L1} (1-D_2) \quad (12)$$

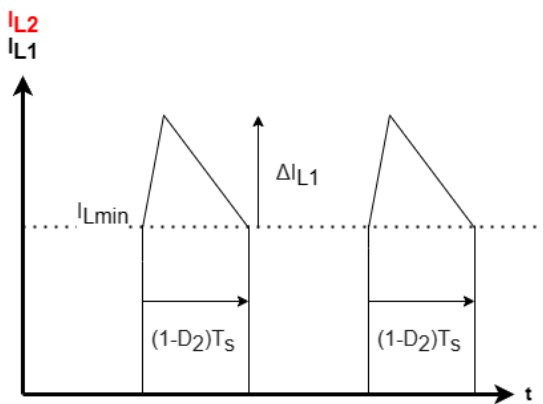


Figure 3 Current present in transistor S_3 .

Source: Own elaboration

Now for the case of $I_{L_{y1}}$ it is taken into account that it is half of I_y ; knowing that the average current in a capacitor is zero, then I_y is the sum of the currents of S_1 and S_2 , and I_{L1} is the sum of S_1 and S_3 so this relation is defined by the next equation.

$$I_{L_{y1}} = \frac{D_2 I_o}{2} \quad (13)$$

IV. Maximum Transistor Voltages and Currents

This is done in order to determine the worst-case stress on the transistors and thus select the most suitable one. For the analysis it should be assumed that the maximum duty cycle D_1 level is 50%. For the voltages in the transistors S_1 - S_4 , it is easy to detect its maximum voltage since it is equal to V_y for all transistors, on the other hand for the current it is taken into account that when the transistor is in conduction, all the inductor current flows through it and because the inductor current is half of the output current, then this would flow through the transistor, only half of the inductor ripple must be added to obtain the maximum current as,

$$I_{S_{max}} = \frac{1}{2} I_{o_{max}} + \frac{V_o}{4L_1 f_s} \quad (14)$$

The maximum voltage across the switches T_1 and T_2 when they are open is equal to the input voltage of V_d ; the capacitors also supply current and have the same voltage as the source, so they supply the same amount of current I_d as the source, so the maximum current is defined as follows,

$$I_{T_{2max}} = I_{T_{1max}} = \frac{1}{4} \frac{N_2}{N_1} I_{o_{max}} \quad (15)$$

From Figure 1 (a) it can be deduced that the maximum stress at T_3 and T_4 is the same as V_s , that is to say $\frac{N_2 V_d}{N_1 2}$. Therefore, the maximum current flowing through these is I_y as expressed as,

$$I_{T_{3max}} = I_{T_{4max}} = \frac{1}{2} I_{o_{max}} + \frac{N_2 V_d}{8N_1 L_{y1} f_s} \quad (16)$$

V. Bidirectional Converter Design

The following design parameters were considered for the calculation of all converter components:

- Input voltage, $V_d=100$ V,
- Output voltage, $V_o=48$ V,
- Switching frequency, $f_s=40$ kHz,
- Output current, $I_o=8.5$ A,
- Current and voltage ripples of 5%,
- Transformer turns ratio, $\frac{N_1}{N_2} = \frac{1}{6}$.

With the equations defined above (1)-(16) it is determine a duty cycle D_1 of 32%, considering that D_2 is always 0.5. Based on the current relations and the current ripple formulas, the inductances of all the coils can be known, which are for L_1 and L_2 a value of 2.82 mH, and for L_{y1} and L_{y2} a value of 15.36 mH, respectively. Finally, the capacitor C_y which is determined to have a value of 18.31 nF.

For the maximum voltages and currents, a duty cycle of 0.5 and an output current of 10 A are assumed. In the Table 1 it is shown the specifications of the voltage and current values of the power semiconductor devices to which they will be subjected in the bidirectional converter.

Although it must be taken into account that in the reverse operation mode (discharge of the supercapacitor), the proposed converter works as a boost and for a maximum input voltage, the duty cycle must be decreased to zero ($D_1 = 0$), but as physically the converters have a limit point where the voltage starts to decrease. For this reason, a duty cycle of 0.1 was selected to calculate the maximum voltages in the reverse direction of the transistors. T_1 , T_2 , T_3 and T_4 , except for the others, since they will work with a fixed duty cycle of 50%.

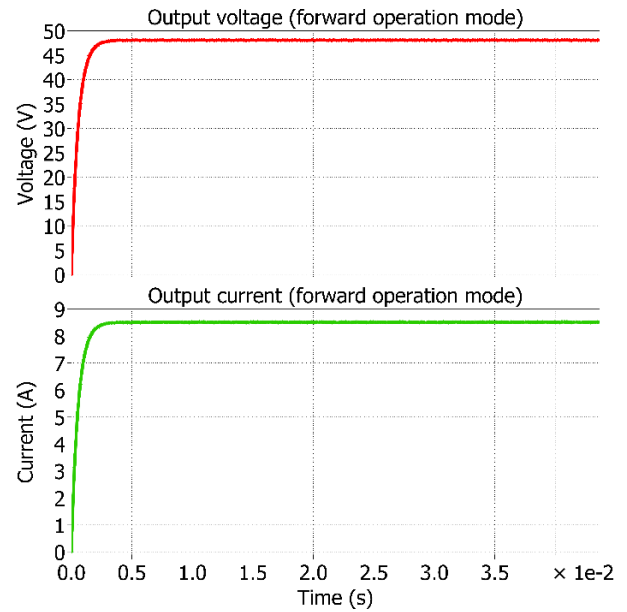
There will be no change in the currents since I_o is assumed as maximum, so a fuse will be used to avoid over currents.

Transistors	Maximum stresses	Peak currents	Maximum stresses (Reverse)
T_1 and T_2	100 V	15 A	320 V
T_3 and T_4	300 V	5.12 A	960 V
S_1 and S_2	150 V	5.16 A	
S_3 and S_4	150 V	5.16	

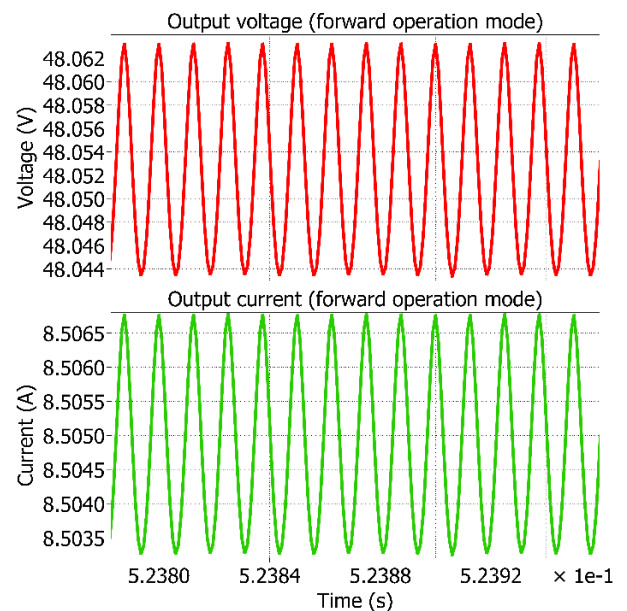
Table 1 Maximum voltages and currents in the converter
Source: Own elaboration

Simulation results

By means of the simulation tool of the PLECS© software, simulation results were performed and obtained, which represent the behavior of the output voltages and currents, as well as of the switches of the proposed converter. These simulations are carried out considering the design parameters and component calculations previously presented. Moreover, it is considered that, during the charging process, the supercapacitor is replaced with a power resistor with a value of 5.65Ω in forward direction. Also, the inductor resistances were considered to be 0.5Ω for the inductors L_y and 0.1Ω for the inductors L .



Graphic 1 Output voltage and current (V_o , I_o respectively)
Source: Own elaboration



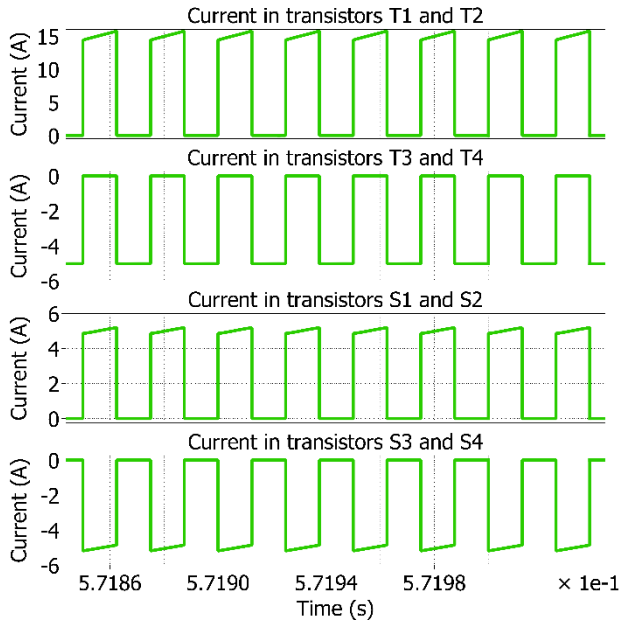
Graphic 2 Ripples in the output voltage and current (forward direction)
Source: Own elaboration

Because the converter is configured for minimum ripple, it can be seen Graphic 1 and Graphic 2 (amplified version of Graphic 1), that the desired voltages and currents are being achieved with a ripple of 0.04% for both.

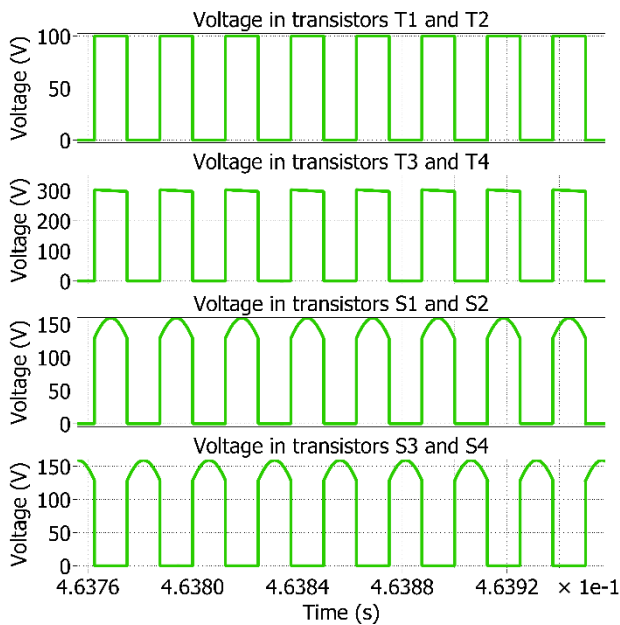
As shown in Graphic 3 and Graphic 4, simulation results confirm that the maximum voltages and currents in the semiconductor devices are similar to those obtained in Table 1.

With this statement, MOSFETs devices can be selected to meet the requirements of the stress voltage and current to which they will be subjected, as well as the switching frequency power semiconductor devices will operate.

In this work, for the switches designated with the letter "T", the semiconductor device CMF10120D was selected, while for the switches designated with the letter "S", the semiconductor device IRF640N was chosen.

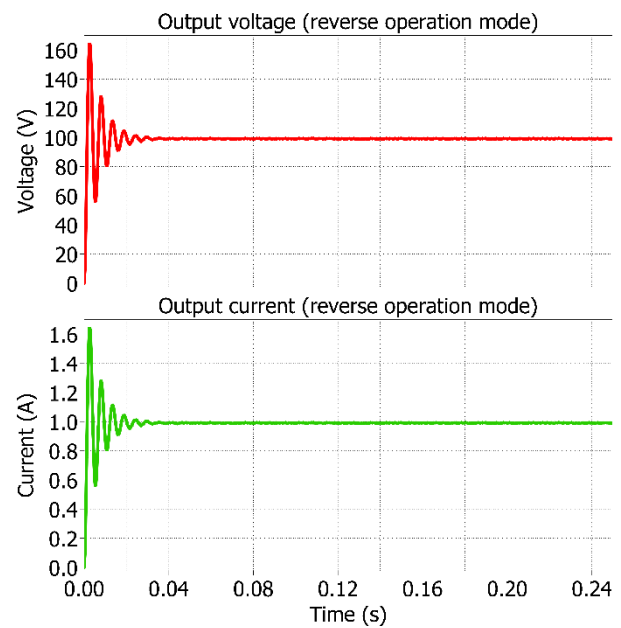


Graphic 3 Simulation results of currents of transistors T1-T4 and S1-S4, as a variation of time
Source: Own elaboration



Graphic 4 Simulation results of voltages of transistors T1-T4 and S1-S4, as a variation of time
Source: Own elaboration

For the case of the reverse operation of the proposed converter, the same duty cycle was used ($D_1 = 0.32$), but the 100 V input source was eliminated and replaced by a 100 Ω power resistor, and the 5.65 Ω was replaced by a 48 V constant voltage source. With the control method by complementary PWMs it is achieved that, for the same duty cycle, the converter is able to operate in two operating directions, as shown in Graphic 5 that prove that can be able to work in discharge mode; Graphic 5 shows the output voltage and current in the resistor of 100 Ω, that is located in the input of the converter.



Graphic 5 Simulation results of the output voltage and current of converter operating in the reverse mode. Source: Own elaboration

Conclusions

In this work, a bidirectional dc-dc converter for charging and discharging applications of ESS systems (e.g. batteries and SCs) was presented. This converter was designed with an approach based on cascading two dc-dc converters. The first one consisted of an isolated half-bridge dc-dc converter with current doubler and the second one of a two-branch stepped parallel bidirectional. Both converters were driven by complementary PWM modulation, where in the first converter a variable duty cycle was used and in the second a fixed 50% duty cycle. The simulation results and the approach used demonstrated that the proposed converter can stabilize the operating voltage and current during the charging and discharging process management of ESS-based applications (e.g. batteries and SCs).

In addition, an effective voltage and current ripple of 0.04% was achieved. This results in a positive impact on the lifetime of ESS systems. Finally, the approach used leads to an easy and practical implementation of the proposed converter in interconnection applications of two power sources with high voltage ratios (e.g. ESS systems and RESs). The latter, due to the implicit advantages offered by the galvanic isolation of the first converter used in the cascade connection.

Acknowledgment

Authors would like to thank Tecnológico Nacional de México (TecNM) for the financial support given to this research project under grant number: 13249.21-P.

References

- Hidalgo-Reyes, J. I., Gómez-Aguilar, J. F., Escobar-Jiménez, R. F., Alvarado-Martínez, V. M., & López-López, M. G. (2019). Classical and fractional-order modeling of equivalent electrical circuits for supercapacitors and batteries, energy management strategies for hybrid systems and methods for the state of charge estimation: A state of the art review. *Microelectronics Journal*, 85, 109–128. <https://doi.org/10.1016/j.mejo.2019.02.006>
- Huang, X., Tang, T., Lv, M., Zhu, Y., & Bao, Q. (2018). Research on the Energy Storage Device of Super Capacitor for Heave Compensation System. *2018 IEEE International Power Electronics and Application Conference and Exposition (PEAC)*, 1–6. <https://doi.org/10.1109/PEAC.2018.8590294>
- Ibanez, F. M., Vadillo, J., Echeverria, J. M., & Fontan, L. (2013). 100kW bidirectional DC/DC converter for a supercapacitor stack. *IEEE PES ISGT Europe 2013*, 1–5. <https://doi.org/10.1109/ISGTEurope.2013.6695246>
- Kayaalp, I., Demirdelen, T., Koroglu, T., Cuma, M. U., Bayindir, K. C., & Tumay, M. (2016). Comparison of Different Phase-Shift Control Methods at Isolated Bidirectional DC-DC Converter. *International Journal of Applied Mathematics, Electronics and Computers*, 4(3), 68. <https://doi.org/10.18100/ijamec.60506>
- Kim, S. M., & Sul, S. K. (2006). Control of rubber tyred gantry crane with energy storage based on supercapacitor bank. *IEEE Transactions on Power Electronics*, 21(5), 1420–1427. <https://doi.org/10.1109/TPEL.2006.880260>
- Lai, C.-M., Yu-Jen Lin, Ming-Hua Hsieh, & Jie-Ting Li. (2016). A newly-designed multiport bidirectional power converter with battery/supercapacitor for hybrid electric/fuel-cell vehicle system. *2016 IEEE Transportation Electrification Conference and Expo, Asia-Pacific (ITEC Asia-Pacific)*, 163–166. <https://doi.org/10.1109/ITEC-AP.2016.7512941>
- Lopez-Flores, D. R., Duran-Gomez, J. L., Herrera-Salcedo, R., & Pineda-Gomez, J. A. (2010). Analysis and design of a simple digital control algorithm for a phase-shift full-bridge DC-DC power converter. *12th IEEE International Power Electronics Congress*, 205–212. <https://doi.org/10.1109/CIEP.2010.5598908>
- Rahimpour, S., & Baghrmian, A. (2017). Bidirectional isolated Γ -source DC-DC converter. *2017 Iranian Conference on Electrical Engineering (ICEE)*, 1378–1383. <https://doi.org/10.1109/IranianCEE.2017.7985257>
- Rico-Secades, M., Lopez-Corominas, E., Calleja, A. J., Quintana, P., Crespo-Iglesias, M., & Garcia-Llera, D. (2016). Improving current equalization in energy storage systems for lighting smart grids applications with the bidirectional one-leg converter. *2016 13th International Conference on Power Electronics (CIEP)*, 339–344. <https://doi.org/10.1109/CIEP.2016.7530781>
- Shreelekha, K., & Arulmozhi, S. (2016). Multiport isolated bidirectional DC-DC converter interfacing battery and supercapacitor for hybrid energy storage application. *2016 International Conference on Electrical, Electronics, and Optimization Techniques (ICEEOT)*, 2763–2768. <https://doi.org/10.1109/ICEEOT.2016.7755198>

Zakis, J., Vinnikov, D., Husev, O., & Rankis, I. (2012). Dynamic behaviour of qZS-based bi-directional DC/DC converter in supercapacitor charging mode. *International Symposium on Power Electronics Power Electronics, Electrical Drives, Automation and Motion*, 764–768. <https://doi.org/10.1109/SPEEDAM.2012.6264554>

Zhixiang Ling, Hui Wang, Kun Yan, & Zaoyi Sun. (2015). A new three-port bidirectional DC/DC converter for hybrid energy storage. *2015 IEEE 2nd International Future Energy Electronics Conference (IFEEC)*, 1–5. <https://doi.org/10.1109/IFEEC.2015.7361598>

[[Title in Times New Roman and Bold No. 14 in English and Spanish]]

Surname (IN UPPERCASE), Name 1st Author†*, Surname (IN UPPERCASE), Name 1st Co-author, Surname (IN UPPERCASE), Name 2nd Co-author and Surname (IN UPPERCASE), Name 3rd Co-author

Institutional Affiliation of Author including Dependency (No.10 Times New Roman and Italic)

International Identification of Science - Technology and Innovation

ID 1st Author: (ORC ID - Researcher ID Thomson, arXiv Author ID - PubMed Author ID - Open ID) and CVU 1st author: (Scholar-PNPC or SNI-CONAHCYT) (No.10 Times New Roman)

ID 1st Co-author: (ORC ID - Researcher ID Thomson, arXiv Author ID - PubMed Author ID - Open ID) and CVU 1st co-author: (Scholar or SNI-CONAHCYT) (No.10 Times New Roman)

ID 2nd Co-author: (ORC ID - Researcher ID Thomson, arXiv Author ID - PubMed Author ID - Open ID) and CVU 2nd co-author: (Scholar or SNI-CONAHCYT) (No.10 Times New Roman)

ID 3rd Co-author: (ORC ID - Researcher ID Thomson, arXiv Author ID - PubMed Author ID - Open ID) and CVU 3rd co-author: (Scholar or SNI-CONAHCYT) (No.10 Times New Roman)

(Report Submission Date: Month, Day, and Year); Accepted (Insert date of Acceptance: Use Only ECORFAN)

Abstract (In English, 150-200 words)

Objectives
Methodology
Contribution

Keywords (In English)

Indicate 3 keywords in Times New Roman and Bold No. 10

Abstract (In Spanish, 150-200 words)

Objectives
Methodology
Contribution

Keywords (In Spanish)

Indicate 3 keywords in Times New Roman and Bold No. 10

Citation: Surname (IN UPPERCASE), Name 1st Author, Surname (IN UPPERCASE), Name 1st Co-author, Surname (IN UPPERCASE), Name 2nd Co-author and Surname (IN UPPERCASE), Name 3rd Co-author. Paper Title. Journal Electrical Engineering. Year 1-1: 1-11 [Times New Roman No.10]

* Correspondence to Author (example@example.org)

† Researcher contributing as first author.

Introduction

Text in Times New Roman No.12, single space.

General explanation of the subject and explain why it is important.

What is your added value with respect to other techniques?

Clearly focus each of its features

Clearly explain the problem to be solved and the central hypothesis.

Explanation of sections Article.

Development of headings and subheadings of the article with subsequent numbers

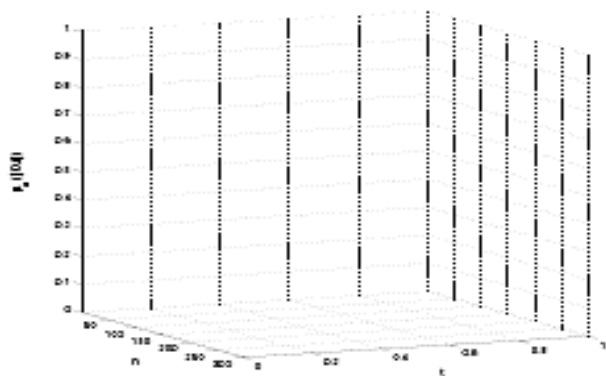
[Title No.12 in Times New Roman, single spaced and bold]

Products in development No.12 Times New Roman, single spaced.

Including graphs, figures and tables-Editable

In the article content any graphic, table and figure should be editable formats that can change size, type and number of letter, for the purposes of edition, these must be high quality, not pixelated and should be noticeable even reducing image scale.

[Indicating the title at the bottom with No.10 and Times New Roman Bold]



Graphic 1 Title and *Source (in italics)*

Should not be images-everything must be editable.



Figure 1 Title and *Source (in italics)*

Should not be images-everything must be editable.

Table 1 Title and *Source (in italics)*

Should not be images-everything must be editable.

Each article shall present separately in **3 folders**: a) Figures, b) Charts and c) Tables in .JPG format, indicating the number and sequential **Bold Title**.

For the use of equations, noted as follows:

$$Y_{ij} = \alpha + \sum_{h=1}^r \beta_h X_{hij} + u_j + e_{ij} \tag{1}$$

Must be editable and number aligned on the right side.

Methodology

Develop give the meaning of the variables in linear writing and important is the comparison of the used criteria.

Results

The results shall be by section of the article.

Annexes

Tables and adequate sources

Thanks

Indicate if they were financed by any institution, University or company.

Conclusions

Explain clearly the results and possibilities of improvement.

References

Use APA system. Should not be numbered, nor with bullets, however if necessary numbering will be because reference or mention is made somewhere in the Article.

Use Roman Alphabet, all references you have used must be in the Roman Alphabet, even if you have quoted an Article, book in any of the official languages of the United Nations (English, French, German, Chinese, Russian, Portuguese, Italian, Spanish, Arabic), you must write the reference in Roman script and not in any of the official languages.

Technical Specifications

Each article must submit your dates into a Word document (.docx):

Journal Name

Article title

Abstract

Keywords

Article sections, for example:

1. Introduction

2. Description of the method

3. Analysis from the regression demand curve

4. Results

5. Thanks

6. Conclusions

7. References

Author Name (s)

Email Correspondence to Author

References

Intellectual Property Requirements for editing:

- Authentic Signature in color of Originality Format Author and Coauthors.
- Authentic Signature in color of the Acceptance Format of Author and Coauthors.

- Authentic Signature in blue color of the Conflict of Interest Format of Author and Coauthors.

Reservation to Editorial Policy

Journal Electrical Engineering reserves the right to make editorial changes required to adapt the Articles to the Editorial Policy of the Research Journal. Once the Article is accepted in its final version, the Research Journal will send the author the proofs for review. ECORFAN® will only accept the correction of errata and errors or omissions arising from the editing process of the Research Journal, reserving in full the copyrights and content dissemination. No deletions, substitutions or additions that alter the formation of the Article will be accepted.

Code of Ethics - Good Practices and Declaration of Solution to Editorial Conflicts

Declaration of Originality and unpublished character of the Article, of Authors, on the obtaining of data and interpretation of results, Acknowledgments, Conflict of interests, Assignment of rights and Distribution

The ECORFAN-Mexico, S.C. Management claims to Authors of Articles that its content must be original, unpublished and of Scientific, Technological and Innovation content to be submitted for evaluation.

The Authors signing the Article must be the same that have contributed to its conception, realization and development, as well as obtaining the data, interpreting the results, drafting and reviewing it. The Corresponding Author of the proposed Article will request the form that follows.

Article title:

- The sending of an Article to Journal Electrical Engineering emanates the commitment of the author not to submit it simultaneously to the consideration of other series publications for it must complement the Format of Originality for its Article, unless it is rejected by the Arbitration Committee, it may be withdrawn.
- None of the data presented in this article has been plagiarized or invented. The original data are clearly distinguished from those already published. And it is known of the test in PLAGSCAN if a level of plagiarism is detected Positive will not proceed to arbitrate.
- References are cited on which the information contained in the Article is based, as well as theories and data from other previously published Articles.
- The authors sign the Format of Authorization for their Article to be disseminated by means that ECORFAN-Mexico, S.C. In its Holding Republic of Peru considers pertinent for disclosure and diffusion of its Article its Rights of Work.
- Consent has been obtained from those who have contributed unpublished data obtained through verbal or written communication, and such communication and Authorship are adequately identified.
- The Author and Co-Authors who sign this work have participated in its planning, design and execution, as well as in the interpretation of the results. They also critically reviewed the paper, approved its final version and agreed with its publication.
- No signature responsible for the work has been omitted and the criteria of Scientific Authorization are satisfied.
- The results of this Article have been interpreted objectively. Any results contrary to the point of view of those who sign are exposed and discussed in the Article.

Copyright and Access

The publication of this Article supposes the transfer of the copyright to ECORFAN-Mexico, S.C. in its Holding Republic of Peru for its Journal Electrical Engineering, which reserves the right to distribute on the Web the published version of the Article and the making available of the Article in This format supposes for its Authors the fulfilment of what is established in the Law of Science and Technology of the United Mexican States, regarding the obligation to allow access to the results of Scientific Research.

Article Title:

Name and Surnames of the Contact Author and the Co-authors	Signature
1.	
2.	
3.	
4.	

Principles of Ethics and Declaration of Solution to Editorial Conflicts

Editor Responsibilities

The Publisher undertakes to guarantee the confidentiality of the evaluation process, it may not disclose to the Arbitrators the identity of the Authors, nor may it reveal the identity of the Arbitrators at any time.

The Editor assumes the responsibility to properly inform the Author of the stage of the editorial process in which the text is sent, as well as the resolutions of Double-Blind Review.

The Editor should evaluate manuscripts and their intellectual content without distinction of race, gender, sexual orientation, religious beliefs, ethnicity, nationality, or the political philosophy of the Authors.

The Editor and his editing team of ECORFAN® Holdings will not disclose any information about Articles submitted to anyone other than the corresponding Author.

The Editor should make fair and impartial decisions and ensure a fair Double-Blind Review.

Responsibilities of the Editorial Board

The description of the peer review processes is made known by the Editorial Board in order that the Authors know what the evaluation criteria are and will always be willing to justify any controversy in the evaluation process. In case of Plagiarism Detection to the Article the Committee notifies the Authors for Violation to the Right of Scientific, Technological and Innovation Authorization.

Responsibilities of the Arbitration Committee

The Arbitrators undertake to notify about any unethical conduct by the Authors and to indicate all the information that may be reason to reject the publication of the Articles. In addition, they must undertake to keep confidential information related to the Articles they evaluate.

Any manuscript received for your arbitration must be treated as confidential, should not be displayed or discussed with other experts, except with the permission of the Editor.

The Arbitrators must be conducted objectively, any personal criticism of the Author is inappropriate.

The Arbitrators must express their points of view with clarity and with valid arguments that contribute to the Scientific, Technological and Innovation of the Author.

The Arbitrators should not evaluate manuscripts in which they have conflicts of interest and have been notified to the Editor before submitting the Article for Double-Blind Review.

Responsibilities of the Authors

Authors must guarantee that their articles are the product of their original work and that the data has been obtained ethically.

Authors must ensure that they have not been previously published or that they are not considered in another serial publication.

Authors must strictly follow the rules for the publication of Defined Articles by the Editorial Board.

The authors have requested that the text in all its forms be an unethical editorial behavior and is unacceptable, consequently, any manuscript that incurs in plagiarism is eliminated and not considered for publication.

Authors should cite publications that have been influential in the nature of the Article submitted to arbitration.

Information services

Indexation - Bases and Repositories

LATINDEX (Scientific Journals of Latin America, Spain and Portugal)

EBSCO (Research Database - EBSCO Industries)

RESEARCH GATE (Germany)

GOOGLE SCHOLAR (Citation indices-Google)

MENDELEY (Bibliographic References Manager)

HISPANA (Information and Bibliographic Orientation-Spain)

Publishing Services

Citation and Index Identification H

Management of Originality Format and Authorization

Testing Article with PLAGSCAN

Article Evaluation

Certificate of Double-Blind Review

Article Edition

Web layout

Indexing and Repository

Article Translation

Article Publication

Certificate of Article

Service Billing

Editorial Policy and Management

1047 La Raza Avenue -Santa Ana, Cusco-Peru. Phones: +52 1 55 6159 2296, +52 1 55 1260 0355, +52 1 55 6034 9181; Email: contact@ecorfan.org www.ecorfan.org

ECORFAN®

Chief Editor

QUINTANILLA-CÓNDOR, Cerapio. PhD

Executive Director

RAMOS-ESCAMILLA, María. PhD

Editorial Director

PERALTA-CASTRO, Enrique. MsC

Web Designer

ESCAMILLA-BOUCHAN, Imelda. PhD

Web Diagrammer

LUNA-SOTO, Vladimir. PhD

Editorial Assistant

TREJO-RAMOS, Iván. BsC

Philologist

RAMOS-ARANCIBIA, Alejandra. BsC

Advertising & Sponsorship

(ECORFAN® Republic of Peru), sponsorships@ecorfan.org

Site Licences

03-2010-032610094200-01-For printed material ,03-2010-031613323600-01-For Electronic material,03-2010-032610105200-01-For Photographic material,03-2010-032610115700-14-For the facts Compilation,04-2010-031613323600-01-For its Web page,19502-For the Iberoamerican and Caribbean Indexation,20-281 HB9-For its indexation in Latin-American in Social Sciences and Humanities,671-For its indexing in Electronic Scientific Journals Spanish and Latin-America,7045008-For its divulgation and edition in the Ministry of Education and Culture-Spain,25409-For its repository in the Biblioteca Universitaria-Madrid,16258-For its indexing in the Dialnet,20589-For its indexing in the edited Journals in the countries of Iberian-America and the Caribbean, 15048-For the international registration of Congress and Colloquiums. financingprograms@ecorfan.org

Management Offices

1047 La Raza Avenue – Santa Ana, Cusco – Peru.

Journal Electrical Engineering

“Implementation of an energy management system based on the ISO 50001 standard in a hospital clinic”

HERNÁNDEZ-RIVERA, Carmen Elizabeth, VIDAL-SANTO, Adrián, MORALES-MARTÍNEZ, Mariel and JASSO-HERNÁNDEZ, Alberto

Universidad Veracruzana

“Application of the disturb and observe algorithm together with a control system for the boost converter in photovoltaic applications”

MÉNDEZ-DÍAZ, Juan Francisco, PERALTA-SÁNCHEZ, Edgar, BONILLA-BARRANCO, Héctor and HERNÁNDEZ-SÁNCHEZ, Daniel Eduardo

*Universidad Popular Autónoma del Estado de Puebla
Instituto Politécnico Nacional*

“Sizing of the photovoltaic system for a house located in the Presa la Concepción subdivision in Santiago Cuautlalpan, State of Mexico”

HERNÁNDEZ-GÓMEZ, Víctor Hugo, MORILLÓN-GÁLVEZ, David, OLVERA-GARCÍA, Omar and GUZMAN-TINAJERO, Pedro

Universidad Nacional Autónoma de México

“Design of a bidirectional converter for charging/discharging a supercapacitor”

GARZA-GONZÁLEZ, Williams, DURÁN-GÓMEZ, José Luis, LÓPEZ-FLORES, David Ricardo and SÁENZ-VALVERDE, David Alberto

Tecnológico Nacional de México campus Chihuahua

